Received: 21 April 2020 | Revised: 17 December 2020 | Accepted: 3 March 2021 | Published on: 9 April 2021

DOI: 10.1002/net.22038

RESEARCH ARTICLE

WILEY

Combinatorial acyclicity models for potential-based flows

Oliver Habeck | **Marc E. Pfetsch**

Department of Mathematics, TU Darmstadt, Darmstadt, Germany

Correspondence
Marc E. Pfetsch, Department of Mathematics, TU Darmstadt, Darmstadt, Germany.
Email: pfetsch@opt.tu-darmstadt.de

Abstract

Potential-based flows constitute a basic model to represent physical behavior in networks. Under natural assumptions, the flow in such networks must be acyclic. The goal of this article is to exploit this property for the solution of corresponding optimization problems. To this end, we introduce several combinatorial models for acyclic flows, based on binary variables for flow directions. We compare these models and introduce a particular model that tries to capture acyclicity together with the supply/demand behavior. We analyze properties of this model, including variable fixing rules. Our computational results show that the usage of the corresponding constraints speeds up solution times by about a factor of 3 on average and a speed-up of a factor of almost 5 for the time to prove optimality.

KEYWORDS

acyclic flows, gas networks, mixed-integer program, network optimization, potential-based flows, valid inequalities

1 | INTRODUCTION

Potential-based flows form a basic model for physical networks. Such flows are necessarily acyclic, which we will exploit in this article. To introduce the basic idea, let $\mathcal{D} = (\mathcal{V}, \mathcal{A})$ be a simple directed graph without antiparallel arcs. For all arcs $a \in \mathcal{A}$, there is a continuous, strictly increasing *potential function* $\psi_a : \mathbb{R} \to \mathbb{R}$ with $\psi_a(0) = 0$ as well as a *resistance* $\beta_a > 0$. Each node $v \in \mathcal{V}$ has an associated *potential* π_v. Under mild assumptions on the potential functions and given demand on the nodes, the defining equations

$$\beta_a\, \psi_a(x_a) = \pi_u - \pi_v \quad \forall\, a = (u, v) \in \mathcal{A}, \tag{1}$$

induce a unique flow $x \in \mathbb{R}^{\mathcal{A}}$ and unique potentials, if one potential is fixed in each connected component (see Section 2). For physical networks, the potentials π_u correspond to quantities like squared pressure or voltage. Note that a directed instead of undirected graph $\mathcal{D}$ is used to define a direction of the flow and (1). Thus, flow values can also be negative, indicating flow in the opposite direction of the arc.

A flow $x \in \mathbb{R}^{\mathcal{A}}$ defines a directed graph $\mathcal{D}(x) = (\mathcal{V}, \mathcal{A}(x))$ with

$$\begin{aligned} \mathcal{A}(x) :=& \{(u, v) \in V \times V \ : \ (u, v) \in \mathcal{A} \ \text{with} \ x_{(u,v)} > 0\} \\ & \cup \{(v, u) \in V \times V \ : \ (u, v) \in \mathcal{A} \ \text{with} \ x_{(u,v)} < 0\}. \end{aligned}$$

If x satisfies (1), this graph is always acyclic. To see this, assume that there would exist a directed cycle $C \subseteq \mathcal{A}(x)$. Then splitting the arcs in C into forward arcs, that is, those contained in the original graph, and backward arcs, that is, those which have the opposite direction to the original graph, we obtain

$$\sum_{(u,v)\in C\cap\mathcal{A}} \beta_{(u,v)}\ \psi_{(u,v)}(x_{(u,v)}) - \sum_{(u,v)\in C\setminus\mathcal{A}} \beta_{(v,u)}\ \psi_{(v,u)}(x_{(v,u)})$$
$$= \sum_{(u,v)\in C\cap\mathcal{A}} \pi_u - \pi_v + \sum_{(u,v)\in C\setminus\mathcal{A}} \pi_u - \pi_v = 0,$$

where we use that C is a cycle and thus the alternating sum of the potentials vanishes. However, since the resistances β_a are positive and each ψ_a is strictly increasing with $\psi_a(0) = 0$, we have $\beta_a\ \psi_a(x_a) > 0$ if $x_a > 0$ and $\beta_a\ \psi_a(x_a) < 0$ if $x_a < 0$. Thus, the value of the first line is positive, leading to a contradiction. This shows that $\mathcal{D}(x)$ is acyclic, corresponding to the physical property of having a conservative potential.

Uniqueness and acyclicity are two important physical properties that are captured by potential-based flows. Moreover, this model class is important for handling energy networks; see Section 2 for examples. Such networks often contain *active* network elements like switches/valves, allowing to close a connection, or generators/pumps/compressors, which can increase the potential on certain arcs. These elements allow to control flow and potentials. Their presence may violate acyclicity, which provides more freedom to control the network. However, the passive components remaining after removal of active elements satisfy acyclicity. We will discuss in Section 4 how we treat active elements, and restrict attention to passive networks until then.

Using the degrees of freedom of active elements and the choice of one potential in each connected component leads to several different optimization problems over such networks, for example, energy minimal operation under the assumption that a given flow demand and potential bounds are satisfied. When solving such optimization problems to global optimality, one can exploit the fact that the passive components of the network still have an acyclic flow. This is the main idea of this article. We will demonstrate how to enhance existing mixed-integer nonlinear programing (MINLP) formulations using binary variables for the flow directions and constraints that enforce acyclicity.

To this end, we introduce a nested sequence of polytopes that encode the acyclicity of the directions of the flows, relaxing more and more constraints of the nonlinear model of potential-based flows along the way. Each of these polytopes provides a combinatorial model of acyclic flows, since they are only based on the binary variables. In Section 3.1, we analyze the relative strengths of these polytopes. The largest polytope (providing the weakest relaxation) is the well-known acyclic subgraph polytope; see Section 3.2 for a discussion.

In Sections 3.3, 3.4, and 3.5, we investigate a particular model that provides a good compromise between the nonlinear model and the acyclic subgraph polytope in more detail. Since it turns out that this polytope has a quite complicated structure, we concentrate on its dimension and how variables can be fixed. Some of the obtained results are similar to ones present in the literature (see also the literature review below).

In Section 4, we then add the corresponding inequalities to a potential-based network optimization problem for gas network examples. It turns out that using binary flow variables and these inequalities allow for a significant strengthening of the variable bounds and fixings of flow directions. Moreover, we demonstrate that this approach leads to an improvement of the total solving time by about a factor of 3 on average. For feasible instances that we can solve to optimality, the solving time improved by almost a factor of 5.

This article is structured as follows. In Section 2, we discuss potential-based flows in more detail and provide examples. Section 3 first introduces the sequence of combinatorial models. Their relation is studied in Section 3.1. In Section 3.2, we investigate a model solely based on acyclic directions and the corresponding computational complexity. Section 3.3 then introduces our main model, exploiting both acyclicity and the fact that one needs to connect sources and sinks. This model is investigated in Sections 3.4 and 3.5 in more detail. Then Section 4 presents the computational results. We close with a conclusion and some open questions in Section 5.

1.1 | Literature review

Potential-based flows have been used in many different contexts. Hendrickson and Janson [20] provide an overview. We will refer to more literature in Section 2 and also discuss examples there. The special case of gas transport will be used in our computations in Section 4.

The topic of acyclic flows in the potential-based setting has been investigated by Becker and Hiller in four articles [3–5, 21]. Their motivation is similar to ours and they also test their methods on gas networks. The main combinatorial model of these articles is based on so-called acyclic source transshipment sink (ASTS) orientations. We will arrive at an equivalent definition through a polyhedral approach in Section 3.3. Their contributions can be briefly summarized as follows. A characterization of the cases in which an ASTS orientation exists is given in [4]. Moreover, various decomposition results based on 2-connected components are presented in [3, 5]. This allows us preprocess the networks [3, Section 3]. The enumeration of ASTS orientations is discussed in [3, 5]. This is used in a Dantzig–Wolfe-type approach to strengthen potential-based flow formulations for gas networks [3, 5].

Our results differ from the ones by Becker and Hiller in the following way. We embed the common combinatorial model in a sequence of polytopes, which we investigate polyhedrally. We use a different binary encoding (see Remark 4), provide a different setup, investigate complexity results, and add the inequalities to the model instead of using enumeration of the configurations. Moreover, we consider the complete graph, whereas the Dantzig–Wolfe approach of Becker and Hiller uses enumerations of acyclic orientations of subgraphs.

The ideas of this article were used for the computations of [19], which was prepared independently of [3–5, 21], and we provide the background in this article. Apart from the mentioned literature, we are not aware of any other works concerning combinatorial models for acyclic flows.

2 | POTENTIAL-BASED FLOWS

Potential-based flows have been studied repeatedly in the literature. It seems that the first appearance is in Birkhoff and Diaz [7]. A general treatment appears in Rockafellar [36]. Before referring to more results in the literature, we first complete the setting of potential-based flows.

Recall that we assume that $\mathcal{A}$ contains at most one of (u, v) and (v, u) for every pair of nodes $u, v \in \mathcal{V}$. For a subset $U \subseteq \mathcal{V}$, we write $\delta^+(U) := \{(u, w) \in \mathcal{A} \ : \ u \in U, w \notin U\}$ for the outgoing arcs and $\delta^-(U) := \{(w, u) \in \mathcal{A} \ : \ u \in U, w \notin U\}$ for the ingoing arcs. We use the abbreviation $\delta^+(v) := \delta^+(\{v\})$ and $\delta^-(v) := \delta^-(\{v\})$ for $v \in \mathcal{V}$.

For every node $v \in \mathcal{V}$, there are lower and upper pressure bounds $\underline{\pi}_v \in \mathbb{R}$ and $\overline{\pi}_v \in \mathbb{R}$, respectively, with $\underline{\pi}_v \leq \overline{\pi}_v$. Additionally, for every arc $a \in \mathcal{A}$, there are lower and upper flow bounds $\underline{x}_a \in \mathbb{R}$ and $\overline{x}_a \in \mathbb{R}$, respectively, with $\underline{x}_a \leq \overline{x}_a$. Let $b \in \mathbb{R}^{\mathcal{V}}$ be a supply and demand vector that is *balanced*, that is, $\sum_{v \in \mathcal{V}} b_v = 0$. A node $v \in \mathcal{V}$ is called *source node* if $b_v > 0$, *sink node* if $b_v < 0$, and *inner node* if $b_v = 0$. Then $(x, \pi) \in \mathbb{R}^{\mathcal{A}} \times \mathbb{R}^{\mathcal{V}}$ is a (passive) *potential-based flow* if it satisfies the following constraints:

$$\sum_{a \in \delta^+(v)} x_a - \sum_{a \in \delta^-(v)} x_a = b_v \qquad \forall v \in \mathcal{V}, \tag{2a}$$

$$\pi_u - \pi_v = \beta_a \ \psi_a(x_a) \qquad \forall a = (u, v) \in \mathcal{A}, \tag{2b}$$

$$\underline{\pi}_v \leq \pi_v \leq \overline{\pi}_v, \qquad \forall v \in \mathcal{V}, \tag{2c}$$

$$\underline{x}_a \leq x_a \leq \overline{x}_a, \qquad \forall a \in \mathcal{A}. \tag{2d}$$

We call $x \in \mathbb{R}^{\mathcal{A}}$ a *b-flow* if it satisfies (2a).

Throughout this article, we will assume that each potential function $\psi_a \ : \ \mathbb{R} \to \mathbb{R}$, $a \in \mathcal{A}$, is continuous and strictly increasing with $\psi_a(0) = 0$. For some results in the literature, additional requirements on the potential functions are needed, for example, that they are odd (i.e., $\psi_a(x) = -\psi_a(-x)$), positively homogeneous (i.e., $\psi_a(\lambda x) = \lambda^r \psi_a(x)$ for all $x \in \mathbb{R}$ and $\lambda > 0$ with some constant $r > 0$) or that they are the same for every arc; see, for example, [16].

One important result (see Maugis [29], Collins et al. [9], and Ríos-Mercado et al. [35]) is the following: Assume that $\mathcal{D}$ is weakly connected, there are no bounds on the potentials and flows, for a given node $s \in \mathcal{V}$ the potential π_s is fixed, and the potential functions are continuous and strictly increasing. Then there exists a unique feasible potential-based flow (x, π). Consequently, System (2) with a fixed potential π_s is either infeasible or has a unique solution. One tool for proving uniqueness is a cost minimal flow problem with a strongly convex objective, whose dual multipliers provide the potentials; see Maugis [29], Rockafellar [36], and [16] for more information and a discussion of the corresponding Lagrange dual.

Example 1. Several interesting applications can be modeled as potential-based flows; see, for example, Hendrickson and Janson [20]. We present three energy network examples:

1. Stationary gas transport networks: Here arcs correspond to pipe(lines), the potentials are the squares of pressures, and flows are gas mass flows. One common approximation of gas flow is (1) with $\psi_a(x_a) = |x_a| \ x_a$. The positive arc-specific constant β_a depends on the pipe diameter, length, and roughness of its inner wall. More details on stationary gas flow in pipeline networks are given in the book [24] and the references therein. The above model assumes constant heights of the network, but one can use scaling to incorporate different heights; see [16].
   The computational results in Section 4 are based on gas networks, extended by active elements like valves and compressors.
2. Water networks: Here potentials correspond to hydraulic heads. Common potential functions are $\psi_a(x_a) = \operatorname{sgn}(x_a) \ |x_a|^{1.852}$ (see, for example, Larock et al. [27]) or $\psi_a(x_a) = |x_a| \ x_a$ (see, for example, Burgschweiger et al. [8]).
3. Lossless DC power flow networks: In this case, the potentials are voltages and the potential function is linear $\psi_a(x_a) = x_a$. For more information about power flow network planning, we refer to Bienstock [6].

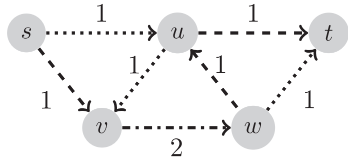

FIGURE 1 An s–t-flow which can be decomposed into two paths (indicated by dashed/dotted arcs) each with flow value 1, but is not acyclic

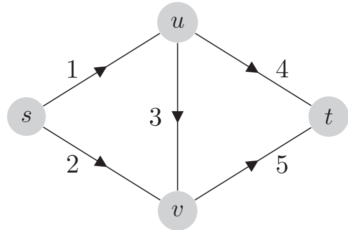

FIGURE 2 A diamond shaped network, with source s and sink t and arc labels 1–5

3 | COMBINATORIAL MODELS FOR ACYCLIC FLOWS

To study acyclic flows, we first introduce some basic notation. Consider the simple and weakly connected directed graph $\mathcal{D}$ without antiparallel arcs. Note that these assumptions are mainly for ease of notation and presentation. Moreover, loops always have a zero flow and can be removed, antiparallel arcs can be reoriented to be parallel and each weakly connected component can be treated separately. Furthermore, if we assume that all arcs have the same positively homogeneous potential function—which is the case for the three examples of energy networks above—parallel arcs can be merged into one arc with adapted β-value; see [16].

We will use $\overleftarrow{a}$ to denote the reverse arc of some arc $a \in \mathcal{A}$, that is, if $a = (u, v)$, then $\overleftarrow{a} := (v, u)$. Furthermore, let $\overleftarrow{\mathcal{A}} := \{\overleftarrow{a} : a \in \mathcal{A}\}$ be the set of the reversed arcs. Note that for a given flow x, we can also write

$$\mathcal{A}(x) = \{a \in \mathcal{A} : x_a > 0\} \cup \{\overleftarrow{a} \in \overleftarrow{\mathcal{A}} : x_a < 0\},$$

and the digraph $\mathcal{D}(x) = (\mathcal{V}, \mathcal{A}(x))$ is a reorientation of the subgraph consisting of arcs with nonzero flow such that all arcs point in the direction of the flow. We say that x is *an acyclic flow* if $\mathcal{D}(x)$ is acyclic. An alternative definition for acyclic flows is given by Hiller and Becker [21, definition 1].

Remark 2. Note that an acyclic s–t-flow does not imply that all flow decompositions only consist of paths and no cycles. On the one hand, the sum of flow along paths can contain a cycle. For example, consider the flow network given in Figure 1. The s–t-flow depicted in this figure can be decomposed into the flows x^1 (dashed) and x^2 (dotted). Both x^1 and x^2 are flows along paths and therefore acyclic, nevertheless their sum is not, since $\mathcal{D}(x^1 + x^2)$ contains the directed cycle $C = (u, v, w, u)$. On the other hand, the sum of flows along paths and cycles can be acyclic. For example consider flow x^3 with value -1 along C. Then, $\mathcal{D}(x^1 + x^2 + x^3)$ is acyclic.

The following example shows how flow directions can depend on the resistances β_a.

Example 3. Consider the potential network given in Figure 2 with source s and sink t and $b_s = -b_t > 0$. Let $b_u = b_v = 0$.

By constraint (2a), it is clear that $x_1 + x_2 = x_4 + x_5 = b_s > 0$ has to hold for every potential flow (x, π). Furthermore, x_1, x_2, x_4, and x_5 have to be nonnegative: Assume that one of them is negative. We can w.l.o.g. assume $x_2 < 0$ by symmetry. Then $x_1 > 0$ by flow conservation. Having $x_3 > 0$ would close the cycle (s, u, v, s). Thus, $x_3 \leq 0$ and by flow conservation $x_5 < 0$. Since also $x_4 > 0$, this closes a cycle (s, u, t, v, s).

Thus, except for arc (u, v), all flow directions for this potential network are fixed, independently of the ψ_a and the β-values. However, the flow direction of (u, v) depends on the ψ_a and the β-values. Indeed, if all β-values and all $\psi = \psi_a$ are equal, then the corresponding flow is $x_3 = 0$. Moreover, consider the case $\beta_1 > \beta_2 = \cdots = \beta_5$ and assume $x_3 \geq 0$. Then $\pi_u \geq \pi_v$ holds by (2b). Furthermore, $\beta_1 > \beta_2$ implies $x_2 > x_1$. Due to flow conservation also $x_5 > x_4$. This gives

$$\pi_t = \pi_u - \beta_4\ \psi(x_4) > \pi_v - \beta_5\ \psi(x_5) = \pi_t,$$

which is a contradiction. Hence, $x_3 < 0$. Furthermore, by symmetry $\beta_1 < \beta_2 = \cdots = \beta_5$ implies $x_3 > 0$. □

To express acyclicity, we introduce binary variables z_a^+ and z_a^- for each arc $a \in \mathcal{A}$ that model the flow direction as follows:

$$\operatorname{sgn}(x_a) = z_a^+ - z_a^-, \quad z_a^+ + z_a^- \leq 1, \tag{3}$$

where $\operatorname{sgn}(x_a) = -1$ if $x_a < 0$, $\operatorname{sgn}(x_a) = 0$ if $x_a = 0$, and $\operatorname{sgn}(x_a) = 1$ if $x_a > 0$. Thus, these constraints imply that $z_a^+ = 1$ if $x_a > 0$, $z_a^- = 1$ if $x_a < 0$, and $z_a^+ = z_a^- = 0$ if $x_a = 0$.

The total model for potential-based flows is the following:

$$\begin{aligned}
\sum_{a\in\delta^+(v)} x_a - \sum_{a\in\delta^-(v)} x_a &= b_v && \forall\, v \in \mathcal{V},\\
\pi_u - \pi_v &= \beta_a\, \psi_a(x_a) && \forall\, a = (u,v) \in \mathcal{A},\\
\underline{\pi}_v \leq \pi_v &\leq \overline{\pi}_v && \forall\, v \in \mathcal{V},\\
\underline{x}_a \leq x_a &\leq \overline{x}_a && \forall\, a \in \mathcal{A},\\
z_a^+ - z_a^- &= \operatorname{sgn}(x_a) && \forall\, a \in \mathcal{A},\\
z_a^+ + z_a^- &\leq 1 && \forall\, a \in \mathcal{A},\\
z_a^+, z_a^- &\in \{0,1\} && \forall\, a \in \mathcal{A}.
\end{aligned} \tag{PBF}$$

Define the feasible set

$$\mathcal{X} := \{(x, \pi, z^+, z^-) \text{ feasible for (PBF)}\} \subset \mathbb{R}^{\mathcal{A}} \times \mathbb{R}^{\mathcal{V}} \times \{0,1\}^{2\mathcal{A}}.$$

Moreover, for $(z^+, z^-) \in \{0,1\}^{2\mathcal{A}}$ we define

$$\mathcal{A}(z^+, z^-) := \{a \in \mathcal{A} \;:\; z_a^+ = 1\} \cup \{\overleftarrow{a} \in \overleftarrow{\mathcal{A}} \;:\; z_a^- = 1\}$$

and the corresponding subgraph $\mathcal{D}(z^+, z^-) := (\mathcal{V}, \mathcal{A}(z^+, z^-))$ of $\overleftrightarrow{\mathcal{D}} := (\mathcal{V}, \overleftrightarrow{\mathcal{A}})$, where $\overleftrightarrow{\mathcal{A}} := \mathcal{A} \cup \overleftarrow{\mathcal{A}}$. Then (z^+, z^-) is *acyclic* if and only if $\mathcal{D}(z^+, z^-)$ is acyclic in the directed sense.

In order to exploit acyclicity of potential-based flows, we will investigate purely combinatorial models of acyclicity, that is, polytopes that are only based on the variables z_a^+ and z_a^-. There are several possibilities for such models, depending on how many properties of the potential-based flow are used. We present four polytopes in the following and one model in Section 3.3. The main goal is to derive inequalities that can be added to (PBF) in order to improve the computational solving performance.

3.1 | Projected potential-based flows

The most specific model considers the projection of feasible points of (PBF) for a given network with given balanced $b \in \mathbb{R}^{\mathcal{V}}$ and yields the *polytope of potential-based flow directions*

$$\mathcal{P}^{\mathrm{PF}} := \operatorname{conv}\left\{ \begin{pmatrix} z^+ \\ z^- \end{pmatrix} \in \{0,1\}^{2\mathcal{A}} \;:\; \exists\, (x,\pi) \in \mathbb{R}^{\mathcal{A}} \times \mathbb{R}^{\mathcal{V}} \text{ with } (x, \pi, z^+, z^-) \in \mathcal{X} \right\}.$$

Note that since the flows are unique, (z^+, z^-) is also unique. The only possible variation is whether $\mathcal{P}^{\mathrm{PF}}$ is empty or not. Since it is an NP-hard problem to decide whether there exists a potential-based flow for the case of DC-flows, see Lehmann et al. [28], and for the case of gas networks, see Szabó [41], it is an NP-hard problem to decide whether $\mathcal{P}^{\mathrm{PF}}$ is empty.

3.2 | Projected universal potential-based flows

Example 3 shows that the flow directions can depend on the values of β. We therefore investigate a model in which the resistances β are allowed to vary.

Consider the asymptotic behavior of $\beta_a^{-1}(\pi_u - \pi_v) = \psi_a(x_a)$ for $\beta_a \to \infty$. For fixed potentials and $\beta_a \to \infty$ we get $x_a \to 0$. Thus, we identify (2b) for $\beta_a = \infty$ with the constraint $x_a = 0$ and decoupled potentials π_u, π_v. This has the same effect as if arc $a = (u, v)$ would not exist. In the following, we denote the extended real line with $\overline{\mathbb{R}} := \mathbb{R} \cup \{\infty\}$.

Again given a digraph $\mathcal{D}$ with balanced $b \in \mathbb{R}^{\mathcal{V}}$, we define the *polytope of universal potential-based flow directions* for (PBF) as

$$\mathcal{P}^{\mathrm{UPF}} := \operatorname{conv}\left\{ \begin{pmatrix} z^+ \\ z^- \end{pmatrix} \in \{0,1\}^{2\mathcal{A}} \;:\; \exists\, \beta \in \overline{\mathbb{R}}_{>0}^{\mathcal{A}}, (x,\pi) \in \mathbb{R}^{\mathcal{A}} \times \mathbb{R}^{\mathcal{V}} \text{ with } (x, \pi, z^+, z^-) \in \mathcal{X} \right\}.$$

By allowing the resistances β to vary, $\mathcal{P}^{\mathrm{UPF}}$ abstracts from the particular network to some extent. Note that the polytope is universal in the sense that changes in β allow a corresponding change of direction of some arcs as in Example 3.

3.3 | Acyclic flows

The *polytope of acyclic flow directions* is

$$\mathcal{P}^{\mathrm{AF}} := \operatorname{conv}\left\{ \begin{pmatrix} z^+ \\ z^- \end{pmatrix} \in \{0,1\}^{2\mathcal{A}} \;:\; \exists\, x \in \mathbb{R}^{\mathcal{A}} \text{ s.t. } (2a), (2d), (3), \mathcal{D}(x) \text{ acyclic} \right\}.$$

Note that the potential equation (2b) of (PBF) is relaxed. Because of (3), we could replace the requirement that $\mathcal{D}(x)$ is acyclic by acyclicity of $\mathcal{D}(z^+, z^-)$.

3.4 | Acyclic subgraphs

The polytope that abstracts the most from potential-based flows is the *polytope of acyclic subgraphs*, see, for example, Grötschel et al. [17]:

$$\mathcal{P}^{\mathrm{AS}} := \operatorname{conv}\left\{ \begin{pmatrix} z^+ \\ z^- \end{pmatrix} \in \{0,1\}^{2\mathcal{A}} \;:\; \mathcal{D}(z^+, z^-) \text{ is acyclic} \right\}. \tag{4}$$

Note that acyclicity of $\mathcal{D}(z^+, z^-)$ implies $z_a^+ + z_a^- \leq 1$ for each arc $a \in \mathcal{A}$. In Section 3.3, we will refine this model by using knowledge of sources, sinks, and inner nodes.

Remark 4. There are two alternatives to using (3). The first one is

$$\underline{x}_a\, z_a^- \leq x_a \leq \overline{x}_a\, z_a^+, \quad z_a^+ + z_a^- \leq 1. \tag{5}$$

These constraints form a relaxation of (3), since the direction variables z_a^+ and z_a^- can be chosen freely if $x_a = 0$ (as long as $z_a^+ + z_a^- \leq 1$). For $(x, \pi, z^+, z^-) \in \mathcal{X}$ this would allow $\mathcal{D}(z^+, z^-)$ to have cycles although $\mathcal{D}(x)$ is acyclic. Thus, $\mathcal{P}^{\mathrm{PF}}$ and $\mathcal{P}^{\mathrm{UPF}}$ would include (z^+, z^-) that do not correspond to potential-based flows. Note that this model is only valid if $\underline{x} \leq 0 \leq \overline{x}$, because positive bounds $\underline{x}$ or negative bounds $\overline{x}$ would be overruled when setting $z^+ = 0$ or $z^- = 0$.

The second alternative for (3) is

$$\underline{x}_a\, z_a^- \leq x_a \leq \overline{x}_a\, z_a^+, \quad z_a^+ + z_a^- = 1.$$

This would require us to also assign directions to 0-flow arcs, which would make the following analysis more difficult. Moreover, we would need to assign a flow direction to an active element like a closed valve/switch, which does not seem natural, and would weaken the relaxations of our combinatorial models discussed in the following. A similar comment holds for models using only one binary variable as in [3, 5].

3.5 | Relations among combinatorial models

The four polytopes introduced above are relaxing more and more of the structure of the nonlinear potential-based flows. Thus, the relaxations become weaker and weaker. Consequently, the following inclusions hold:

$$\mathcal{P}^{\mathrm{PF}} \subseteq \mathcal{P}^{\mathrm{UPF}} \subseteq \mathcal{P}^{\mathrm{AF}} \subset \mathcal{P}^{\mathrm{AS}}.$$

In fact, Example 3 shows that in general the first inclusion is strict. The last inclusion is always strict: on the one hand, if $b \neq 0$, then $0 \notin \mathcal{P}^{\mathrm{AF}}$, but we always have $0 \in \mathcal{P}^{\mathrm{AS}}$; on the other hand, if $b = 0$ then $\mathcal{P}^{\mathrm{AF}} = \{0\}$, but we can always set a single direction to 1 in $\mathcal{P}^{\mathrm{AS}}$.

The following result shows that equality can hold for the remaining inclusion.

Lemma 5. *If there are no potential bounds then $\mathcal{P}^{\mathrm{UPF}} = \mathcal{P}^{\mathrm{AF}}$ holds.*

Proof. If suffices to show $\mathcal{P}^{\mathrm{AF}} \subseteq \mathcal{P}^{\mathrm{UPF}}$. To this end, suppose first that $b = 0$. Then the only acyclic flow satisfying (2a) is $x = 0$. Thus, if $x = 0$ satisfies the flow bounds (2d), $z^+ = z^- = 0$ is the only possible solution and $\mathcal{P}^{\mathrm{UPF}} = \mathcal{P}^{\mathrm{AF}} = \{0\}$ holds.

Otherwise, let $b \neq 0$ be balanced and consider any $(z^+, z^-) \in \mathcal{P}^{\mathrm{AF}} \cap \{0,1\}^{2\mathcal{A}}$. Furthermore, let $x \in \mathbb{R}^{\mathcal{A}}$ be an acyclic b-flow satisfying the flow bounds (2d) and the coupling (3) with the binary variables (z^+, z^-). Note that x with these properties exists by definition of $\mathcal{P}^{\mathrm{AF}}$. To show that $(z^+, z^-) \in \mathcal{P}^{\mathrm{UPF}}$ holds, we have to show that there exist potentials $\pi \in \mathbb{R}^{\mathcal{V}}$ which satisfy $\pi_u - \pi_v = \beta_a\, \psi_a(x_a)$ for all arcs $a = (u, v)$ with appropriately chosen resistances $\beta \in \overline{\mathbb{R}}_{>0}^{\mathcal{A}}$.

We first compute potentials π such that $\pi_u - \pi_v \geq x_a$ if $x_a > 0$ and $\pi_u - \pi_v \leq x_a$ if $x_a < 0$ holds for all arcs $a = (u, v) \in \mathcal{A}$. To this end, consider the digraph

$$\mathcal{D}' = (\mathcal{V} \cup \{r\}, \mathcal{A}(x) \cup \{(r, v) \;:\; v \in \mathcal{V}\})$$

with an artificial node r and additional arcs (r, v) for all $v \in \mathcal{V}$. Furthermore, we define weights w on this graph as follows. We define $w_a = -x_a$ for arcs $a \in \mathcal{A}(x) \cap \mathcal{A}$, $w_a = x_a$ for arcs $a \in \mathcal{A}(x) \cap \overleftarrow{\mathcal{A}}$ and $w_a = 0$ for the additional arcs $a = (r, v)$. Note that by construction $\mathcal{D}'$ does not contain any cycles, because x is acyclic. Thus, the Moore–Bellman–Ford algorithm computes the shortest distances π_v from r to all nodes $v \in \mathcal{V}$ with $\pi_v \leq \pi_u + w_a$ for all $a = (u, v) \in \mathcal{A}(x)$; see, for example, Korte and Vygen [25]. By definition of the weights w, this implies $\pi_u - \pi_v \geq x_a$ if $x_a > 0$ and $\pi_u - \pi_v \leq x_a$ if $x_a < 0$ for all arcs $a = (u, v) \in \mathcal{A}$. Moreover, note that one can shift the potentials such that $\pi \geq 0$ holds.

We now choose β-values such that equation $\pi_u - \pi_v = \beta_a\, \psi_a(x_a)$ holds for each arc $a = (u, v) \in \mathcal{A}$. For an arc a with $x_a = 0$ we choose $\beta_a = \infty$, which corresponds to $x_a = 0$ with decoupled potentials as mentioned when introducing $\mathcal{P}^{\mathrm{UPF}}$. Otherwise, let $x_a \neq 0$. If $x_a > 0$, we can choose $\beta_a := (\pi_u - \pi_v)/\psi_a(x_a) > 0$, since $\pi_u - \pi_v \geq x_a > 0$. Analogously, if $x_a < 0$, we can choose $\beta_a := (\pi_u - \pi_v)/\psi_a(x_a) > 0$ since $\pi_u - \pi_v \leq x_a < 0$ and $\psi_a(x_a) < 0$. ∎

This yields the following result.

Corollary 6. *If no potential bounds are present, $\mathcal{P}^{\mathrm{PF}} \subseteq \mathcal{P}^{\mathrm{UPF}} = \mathcal{P}^{\mathrm{AF}} \subset \mathcal{P}^{\mathrm{AS}}$ and the two inclusions are strict in general.*

The following results justify the possibility to choose $\beta_a = \infty$ in $\mathcal{P}^{\mathrm{UPF}}$. Therefore, given a weakly connected digraph $\mathcal{D} = (\mathcal{V}, \mathcal{A})$ and a balanced supply and demand vector $b \in \mathbb{R}^{\mathcal{V}}$, we define the set of all potential-based flows

$$\mathcal{X}_x := \{x \in \mathbb{R}^{\mathcal{A}} \;:\; \exists\, \beta \in \mathbb{R}^{\mathcal{A}}_{>0}, \pi \in \mathbb{R}^{\mathcal{V}} \text{ with } (x, \pi) \text{ satisfying (2a), (2b)}\}.$$

We first show that in the absence of flow and potential bounds the closure of $\mathcal{X}_x$ is given by permitting $\beta_a = \infty$. Note that $\mathcal{X}_x$ is never empty, since for all $\beta \in \mathbb{R}^{\mathcal{A}}_{>0}$ and any node $v \in \mathcal{V}$ with fixed potential π_v, there exists a unique solution (x, π) of equations (2a) and (2b); see, for example, Maugis [29].

Proposition 7. *Let the potential function ψ be continuous and strictly increasing. Consider a weakly connected digraph $\mathcal{D} = (\mathcal{V}, \mathcal{A})$ and a balanced supply and demand vector $b \in \mathbb{R}^{\mathcal{V}}$. The closure of potential-based flows is given by*

$$\mathrm{cl}(\mathcal{X}_x) = \{x \in \mathbb{R}^{\mathcal{A}} \;:\; \exists\, \beta \in \overline{\mathbb{R}}^{\mathcal{A}}_{>0}, \pi \in \mathbb{R}^{\mathcal{V}} \text{ with } (x, \pi) \text{ satisfying (2a), (2b)}\}. \tag{6}$$

Proof. In the case $b = 0$, both sets only contain $x = 0$. Thus, it suffices to consider the case $b \neq 0$. In the following, we denote the set on the right of (6) by $\mathcal{X}^{\infty}$.

We first show $\mathrm{cl}(\mathcal{X}_x) \subseteq \mathcal{X}^{\infty}$. We assume there exists $x^* \in \mathrm{cl}(\mathcal{X}_x) \setminus \mathcal{X}_x$ as otherwise there is nothing to show. To prove $x^* \in \mathcal{X}^{\infty}$, we have to construct resistances $\beta \in \overline{\mathbb{R}}^{\mathcal{A}}_{>0}$ and potentials π^* such that (x^*, π^*) satisfy (2a) and (2b). If x^* is acyclic, we can use the procedure in the proof of Lemma 5. Thus, we have to show that $\mathcal{A}(x^*)$ is acyclic.

Suppose that $\mathcal{A}(x^*)$ contains a directed cycle C and w.l.o.g. assume that $x^*_a > 0$ for all arcs $a \in C$. Let $(x^{(k)})_{k \in \mathbb{N}} \subset \mathcal{X}_x$ converge to x^*. Then for some k_0, $x^{(k_0)}_a > 0$ holds for all $a \in C$, which contradicts $x^{(k_0)}$ being a potential-based flow. Hence, x^* is acyclic and we conclude that the inclusion $\mathrm{cl}(\mathcal{X}_x) \subseteq \mathcal{X}^{\infty}$ holds.

We now show the reverse inclusion $\mathcal{X}^{\infty} \subseteq \mathrm{cl}(\mathcal{X}_x)$. Let $x^* \in \mathcal{X}^{\infty}$ with corresponding resistances $\beta^* \in \overline{\mathbb{R}}^{\mathcal{A}}_{>0}$ and potentials π^*. If $\beta^* \in \mathbb{R}^{\mathcal{A}}_{>0}$, then we are done by definition. Therefore, assume that $\beta_a = \infty$ for at least one arc $a \in \mathcal{A}$. To finish the proof, we construct a sequence $(x^{(k)})_{k \in \mathbb{N}} \subset \mathcal{X}_x$ converging to x^* as follows:

1 We define a sequence of resistances $(\beta^{(k)})_{k \in \mathbb{N}} \subset \mathbb{R}^{\mathcal{A}}_{>0}$, by using $\beta^{(k)}_a = \beta^*_a$ for all arcs a with $\beta^*_a < \infty$ and $\beta^{(k)}_a = 2^k$ otherwise.
2 Choose a source $s \in \mathcal{V}$ and fix $\pi^{(k)}_s = \pi^*_s$ for all $k \in \mathbb{N}$.
3 Since there are no flow or potential bounds, there exists a unique solution $(x^{(k)}, \pi^{(k)})$ for every $k \in \mathbb{N}$.

We claim that the sequence $x^{(k)}$ constructed this way converges to x^*. To see this, consider the subgraph $\mathcal{D}^{\infty} = (\mathcal{V}^{\infty}, \mathcal{A}^{\infty})$ of $\mathcal{D}$, which results from removing all arcs with $\beta^*_a = \infty$ and all resulting isolated nodes.

Due to flow conservation and the acyclicity of potential-based flows, we can derive lower and upper bounds on the flow of each arc, for example, the flows are bounded by the total sum of inflows. These flow bounds together with (2b) then define a lower and an upper bound on the potential difference between the nodes of each weakly connected component in $\mathcal{D}^{\infty}$.

Let $a = (u, v) \in \mathcal{A} \setminus \mathcal{A}^{\infty}$ and suppose that $x^{(k_0)}_a$ does not converge to 0. Then (a subsequence of) the sequence $\beta^{(k)}_a\, \psi_a(x^{(k)}_a)$ converges to $\pm\infty$. If u, v are in the same connected component of $\mathcal{D}^{\infty}$, this contradicts the potential differences of each component being bounded. Otherwise, note that due to flow conservation there can only be flow from one connected component to another, if there is also flow to the first component from another component, and vice versa. Thus, there exists a "cycle" of arcs in $\mathcal{A} \setminus \mathcal{A}^{\infty}$ connecting different components of $\mathcal{D}^{\infty}$. Hence, if the flow on these arcs does not converge to 0, the potential differences of the nodes where the flow enters and leaves the different components converges to $\pm\infty$, which is a contradiction as before.

To finalize the proof, suppose that (a subsequence of) $x^{(k)}$ converges to some flow $\overline{x} \neq x^*$ with corresponding potentials $\overline{\pi}$. Then there exists a unique potential-based flow on each connected component of $\mathcal{D}^\infty$ if one potential of each component is fixed. However, since shifting all potentials π^* of a connected component by the same amount does not change the feasibility of (2b), we can assume that π^* coincides with $\overline{\pi}$ on at least one node of each connected component. Thus, $\overline{x} \neq x^*$ is a contradiction. ∎

The previous result can also be extended to the case with flow bounds.

Corollary 8. *Using the assumptions of Proposition 7, the following holds. Given flow bounds $\underline{x} \leq \overline{x}$, we define $\mathcal{X}_{[x]} := \mathcal{X}_x \cap [\underline{x}, \overline{x}]$. If $\mathcal{X}_{[x]} \neq \emptyset$, then the closure of $\mathcal{X}_{[x]}$ is*

$$\mathrm{cl}(\mathcal{X}_{[x]}) = \{x \in \mathbb{R}^{\mathcal{A}} \ : \ \exists\, \beta \in \overline{\mathbb{R}}^{\mathcal{A}}_{>0}, \pi \in \mathbb{R}^{\mathcal{V}} \ \textit{with} \ (x,\pi) \ \textit{satisfying} \ \text{(2a), (2b), (2d)}\}.$$

Proof. The inclusion "⊆" holds by the same arguments as before. To see "⊇," we use the same construction to define the sequence $(x^{(k)}, \pi^{(k)})_{k\in\mathbb{N}}$. After possibly choosing a subsequence, all elements of the sequence either satisfy the flow bounds, or all violate the flow bounds. That is, the sequence is either contained in $\mathrm{cl}(\mathcal{X}_{[x]})$ or $\mathrm{cl}(\mathcal{X}_x) \setminus \mathrm{cl}(\mathcal{X}_{[x]})$. In the first case, we are done. Otherwise, note that the flow bounds are satisfied in the limit and thus the limit is not contained in the complement of $\mathrm{cl}(\mathcal{X}_{[x]})$ but in the intersection of the closures. ∎

Remark 9.

- Combining Lemma 5 and Corollary 8 yields that in the absence of potential bounds, acyclic flows coincide with the closure of potential-based flows.
- Instead of taking the closure of the flows only, we could also consider

$$\mathcal{X}_{(x,\pi)} := \{(x,\pi) \in \mathbb{R}^{\mathcal{A}} \times \mathbb{R}^{\mathcal{V}} \ : \ \exists\, \beta \in \mathbb{R}^{\mathcal{A}}_{>0} \ \text{s.t.} \ (x,\pi) \ \text{satisfy (2a), (2b)}\}.$$

  Then the closure satisfies

$$\mathrm{cl}(\mathcal{X}_{(x,\pi)}) \subsetneq \{(x,\pi) \in \mathbb{R}^{\mathcal{A}} \times \mathbb{R}^{\mathcal{V}} \ : \ \exists\, \beta \in \overline{\mathbb{R}}^{\mathcal{A}}_{\geq 0} \ \text{s.t.} \ (x,\pi) \ \text{satisfy (2a), (2b)}\},$$

  where additionally $\beta_a = 0$ is permitted. Here, the reverse inclusion is in general not true, because when using $\beta_a = 0$, flow in a cycle is possible, while potential-based flows are always acyclic.
- Note that taking the closure of potential-based flows together with the corresponding directions defined by (3) does *not* yield the same results as defining the directions after taking the closure of the flows, for example, consider Figure 2. We have seen that $x_1 > 0$ for all $\beta_1 \in \mathbb{R}_{>0}$, and thus $z_1^+ = 1$. But by taking the closure of flows with the direction variables, $x_1 = 0$ is possible, while still $z_1^+ = 1$ holds for all elements of the closure, that is, (3) is violated.
- For energy networks $\beta_a = \infty$ can be interpreted as if the arc is combined with a switch/valve which is turned off/closed. This interpretation might be useful for network design; see, for example, Raghunathan [34].

3.6 | Acyclic subgraphs and computational complexity

We next obtain a complete description of $\mathcal{P}^{\mathrm{AS}}$ if the graph is planar by using known results from the literature. Indeed, acyclic $(z^+, z^-) \in \{0,1\}^{2\mathcal{A}}$ correspond to acyclic subgraphs of the digraph $\overleftrightarrow{\mathcal{D}} = (\mathcal{V}, \overleftrightarrow{\mathcal{A}})$. The corresponding *acyclic subgraph problem* was investigated by Grötschel et al. [17]. The acyclic subgraph polytope is the convex hull of incidence vectors of acyclic arc sets in a given digraph. Grötschel et al. showed that for planar graphs a complete description of the acyclic subgraph polytope is given by the variable bounds and so-called *dicycle inequalities*. These inequalities are based on the set of all dicycles (directed cycles) in $\overleftrightarrow{\mathcal{D}}$:

$$\mathcal{C} := \{C \subseteq \overleftrightarrow{\mathcal{A}} \ : \ C \ \text{directed cycle}\}.$$

Note that the antiparallel arcs $\{a, \overleftarrow{a}\}$ form a particular dicycle in $\overleftrightarrow{\mathcal{D}}$. Thus, translated to our setting, we obtain the following:

Corollary 10 (Grötschel et al. [17]). *If $\overleftrightarrow{\mathcal{D}}$ is planar then*

$$\mathcal{P}^{\mathrm{AS}} = \{(z^+, z^-) \in [0,1]^{2\mathcal{A}} \ : \ \sum_{a\in C} z_a^+ + \sum_{\overleftarrow{a}\in C} z_a^- \leq |C| - 1 \quad \forall\, C \in \mathcal{C}\}. \tag{7}$$

Note that planarity is a reasonable assumption for real-world physical networks. In general networks, however, optimizing over $\mathcal{P}^{\mathrm{AS}}$ is NP-hard.

Lemma 11. *Linear optimization over $\mathcal{P}^{\mathrm{AS}}$ is NP-hard.*

Proof. Grötschel et al. [17] already observed that linear optimization over the acyclic digraph polytope is NP-hard, since finding a maximum acyclic subdigraph is NP-hard—this problem is complementary to the feedback arc set problem, which has been proven to be NP-hard by Karp [23]. We note the graph in the reduction is simple and does not contain antiparallel arcs. When optimizing over $\mathcal{P}^{\mathrm{AS}}$ and considering $\overleftrightarrow{D}$, we can choose the weight to be 0 for either a or $\overleftarrow{a}$, depending on which direction is present in the original digraph. Thus, optimization over the acyclic subgraph polytope is equivalent to optimization over $\mathcal{P}^{\mathrm{AS}}$. ∎

Lemma 12. *Given a directed graph with rational flow bounds and supplies/demands b, it is NP-complete to decide whether there exists an acyclic b-flow.*

Proof. If there exists an acyclic flow, there exists one with polynomial encoding length in the size of the instance. Moreover, acyclicity can be checked in polynomial time. Thus, the problem is in NP.

Consider an instance of the independent set problem: Given an undirected graph $G=(V,E)$ and an integer K, the question is whether there exists an independent subset of nodes of size at least K, that is, no two selected nodes are connected by an edge. Construct the following directed graph $\mathcal{D}=(\mathcal{V},\mathcal{A})$. The node set is

$$\mathcal{V}=\{s,t\}\cup\{v' \;:\; v\in V\}\cup\{v'' \;:\; v\in V\},$$

where s and t are two new nodes and v', v'' are distinct copies of $v\in V$. The arcs in $\mathcal{A}$ are constructed as follows: For each edge $\{u,v\}\in E$ we add two arcs (u'',v') and (v'',u'); the corresponding flow bounds are such that the flow on these arcs is fixed to 1. Moreover, for each node $v\in V$, we add arcs (v',v'') as well as arcs (s,v') and (v'',t); the flow on these arcs is restricted to lie in $[0,1]$. Moreover, we set $b_{v''}=-b_{v'}=\deg(v)$ for each original node $v\in V$ and $b_s=-b_t=K$.

Note that because of the flow bounds, the direction of the flows is fixed. However, x_a can still be 0 on arcs a of type (s,v'), (v',v'') or (v'',t).

Consider an independent set $S\subseteq V$ of size K in G. Then there exists an acyclic flow in $\mathcal{D}$: For each $v\in S$, the arcs (s,v'), (v',v''), and (v'',t) have flow value 1. The arcs (s,v'), (v',v''), and (v'',t) for $v\notin S$ have flow 0. The flow on all other arcs is fixed to 1. It is easy to see that this forms a b-flow. Moreover, it is acyclic. Indeed, because of the flow bounds, the only directed cycles are $(v_1',v_1'',v_2',v_2'',v_1')$ for an edge $\{v_1,v_2\}\in E$ or $(v_1',v_1'',v_2',v_2'',\ldots,v_j',v_j'',v_1')$ for a cycle $(v_1,v_2,\ldots,v_j,v_1)$ in $G=(V,E)$. Since S is independent, the flow on either (v_1',v_1'') or (v_2',v_2'') is 0. Thus, in each cycle there is at least one arc with zero flow.

Conversely, let $x\in\mathbb{R}^{\mathcal{A}}$ be a feasible acyclic b-flow and define the following set of nodes $S:=\{v\in V \;:\; x_{(v',v'')}>0\}$. Because of the demand of $-K$ at t and the flow bounds, we have $|S|\geq K$. Moreover, S is independent. Indeed, if there would exist an edge $\{u,v\}\subseteq S$, then x would contain a cycle (u',u'',v',v'',u'). ∎

As a consequence, we cannot expect to obtain tractable linear descriptions for $\mathcal{P}^{\mathrm{AS}}$ and $\mathcal{P}^{\mathrm{AF}}$ in general graphs.

Obviously, acyclic subgraphs are not an accurate model for the feasible flow directions, for instance, since proper disconnected subgraphs might not even support a feasible flow. Nevertheless, the acyclic subgraph polytope is well investigated and provides a relaxation.

3.7 | Acyclic subgraphs with sources and sinks

To obtain a polytope contained in $\mathcal{P}^{\mathrm{AS}}$, but closer to $\mathcal{P}^{\mathrm{AF}}$, we use the knowledge of sources and sinks in the network. For $b\in\mathbb{R}^{\mathcal{V}}$, define the set of sources $\mathcal{V}_+ := \{v\in\mathcal{V} \;:\; b_v>0\}$, the set of sinks $\mathcal{V}_- := \{v\in\mathcal{V} \;:\; b_v<0\}$, and the inner nodes $\mathcal{V}_0 := \{v\in\mathcal{V} \;:\; b_v=0\}$. Then $\mathcal{V}=\mathcal{V}_+\dot\cup\mathcal{V}_-\dot\cup\mathcal{V}_0$. In the following, for some arc set $S\subseteq\mathcal{A}$ we use the shorthand notation $z^+(S)=\sum_{a\in S}z_a^+$ and $z^-(S)=\sum_{a\in S}z_a^-$.

For $s\in\mathcal{V}_+$, there has to exist at least one arc with flow away from the source s. Similarly, for $t\in\mathcal{V}_-$, there exists at least one arc with flow toward t. This can be expressed via the valid inequalities

$$z^+(\delta^+(s))+z^-(\delta^-(s))\geq 1, \tag{8a}$$

$$z^-(\delta^+(t))+z^+(\delta^-(t))\geq 1. \tag{8b}$$

Furthermore, for every inner node $v\in\mathcal{V}_0$ in- and outflow have to be balanced, because of (2a). That is, if there is flow to v, that is, there is an arc $a\in\delta^-(v)$ with $x_a>0$ or an arc $a\in\delta^+(v)$ with $x_a<0$, there has to exist flow from v to another node, that is, there is an arc $a' \in \delta^-(v)$ with $x_{a'} < 0$ or an arc $a' \in \delta^+(v)$ with $x_{a'} > 0$, and vice versa. Thus, for the binary variables this implies that if there is an arc $(u, v) \in \mathcal{A}(z^+, z^-)$, there has to exist another node w with an incident arc $(v, w) \in \mathcal{A}(z^+, z^-)$, and vice versa. There are several possibilities to represent this by linear inequalities. We introduce two options, which differ in their strength and number of added inequalities.

Given a node $v \in \mathcal{V}_0$, the first option is to add an inequality for both directions of every arc incident to v. The inequalities are

$$z_a^+ \le z^-(\delta^+(v) \setminus \{a\}) + z^+(\delta^-(v)) \qquad \forall\, v \in \mathcal{V}_0, a \in \delta^+(v), \tag{9a}$$

$$z_a^- \le z^+(\delta^-(v) \setminus \{a\}) + z^-(\delta^+(v)) \qquad \forall\, v \in \mathcal{V}_0, a \in \delta^-(v), \tag{9b}$$

$$z_a^- \le z^+(\delta^+(v) \setminus \{a\}) + z^-(\delta^-(v)) \qquad \forall\, v \in \mathcal{V}_0, a \in \delta^+(v), \tag{9c}$$

$$z_a^+ \le z^-(\delta^-(v) \setminus \{a\}) + z^+(\delta^+(v)) \qquad \forall\, v \in \mathcal{V}_0, a \in \delta^-(v). \tag{9d}$$

Here, the first two inequalities imply that if arc a incident to v is oriented away from v, then there has to exist another arc that is oriented toward v. The other two inequalities imply the converse. This discrete representation of flow conservation requires $2\sum_{v\in\mathcal{V}_0} \deg(v)$ inequalities.

Another option is to aggregate the first two inequalities and the last two inequalities, which yields

$$z^+(\delta^+(v)) + z^-(\delta^-(v)) \le (\deg(v) - 1)(z^-(\delta^+(v)) + z^+(\delta^-(v))), \tag{10a}$$

$$z^-(\delta^+(v)) + z^+(\delta^-(v)) \le (\deg(v) - 1)(z^+(\delta^+(v)) + z^-(\delta^-(v))). \tag{10a}$$

Again the first inequality implies that if there is an outgoing arc of node v, there has to exist an incoming arc, while the second inequality implies the converse. This representation usually has fewer inequalities: $2\,|\mathcal{V}_0|$ instead of $2\sum_{v\in\mathcal{V}_0} \deg(v)$. However, while both variants allow for the same integral points, the following example shows that they differ in the strength of their LP-relaxations.

Example 13. Consider again the graph shown in Figure 2 with $b_s = -b_t > 0$ and $b_u = b_v = 0$. Here, $z_1^+ = 1$, $z_3^+ = \frac{1}{2}$, $z_5^+ = 1$, and the remaining variables equal to 0 is feasible for the inequalities (10). In fact, it is a vertex of the LP-relaxation of (7) with the additional constraints (8) and (10). However, this solution is not feasible for (9). Furthermore, all feasible solutions of (9) are feasible for (10). This shows that the first option yields tighter LP-relaxations.

Note that for this and subsequent examples we used polymake [2, 14] to enumerate integer points, compute vertices, dimension, affine hull, and facets of polytopes.

In the following we will therefore concentrate on (9) and investigate the formulation given by these inequalities as well as the dicycle inequalities

$$\sum_{a\in C} z_a^+ + \sum_{\overleftarrow{a}\in C} z_a^- \le |C| - 1 \quad \forall\, C \in \mathcal{C}. \tag{11}$$

We define the *polytope of acyclic flows with sources and sinks* as

$$\mathcal{P}^{\mathrm{AS}\pm} := \operatorname{conv}\left\{(z^+, z^-) \in \{0,1\}^{2\mathcal{A}} \;:\; (z^+, z^-) \text{ is feasible for } (8), (9), (11)\right\}. \tag{12}$$

We will also need the LP-relaxation corresponding to $\mathcal{P}^{\mathrm{AS}\pm}$:

$$\mathcal{P}^{\mathrm{AS}\pm}_{\mathrm{LP}} := \left\{(z^+, z^-) \in [0,1]^{2\mathcal{A}} \;:\; (z^+, z^-) \text{ satisfying } (8), (9), (11)\right\}.$$

The model derived here turns out to be equivalent to the one investigated by Becker and Hiller [3, 4, 21], which can be seen using the analysis in the next section.

3.8 | Analysis of acyclic subgraphs with sources and sinks

In this section we analyze the polytope $\mathcal{P}^{\mathrm{AS}\pm}$ and its relation to $\mathcal{P}^{\mathrm{AF}}$. We start by proving a key insight, which helps to derive several results in the following. Note that we define paths to be *simple*, that is, no node appears twice in the path. We call a directed path a *source–sink-path* if it starts in $\mathcal{V}_+$ and ends in $\mathcal{V}_-$.

Proposition 14. *Let $(z^+, z^-) \in \mathcal{P}^{\mathrm{AS}\pm} \cap \{0,1\}^{2\mathcal{A}}$. For every arc in $\mathcal{A}(z^+, z^-)$, there exists a directed source–sink-path containing this arc. In particular, $\mathcal{D}(z^+, z^-)$ contains at least one path leaving each node in $\mathcal{V}_+$ and at least one path entering each node of $\mathcal{V}_-$. Moreover, if $b = 0$, then $\mathcal{P}^{\mathrm{AS}\pm} = \{0\}$.*

Proof. Consider an arbitrary arc $a = (u, v) \in \mathcal{A}(z^+, z^-)$. We construct a path from v to $\mathcal{V}_-$ and a path from $\mathcal{V}_+$ to u, which together with a yield the desired path. Note that these three paths are necessarily simple, since otherwise $\mathcal{A}(z^+, z^-)$ contains a cycle.

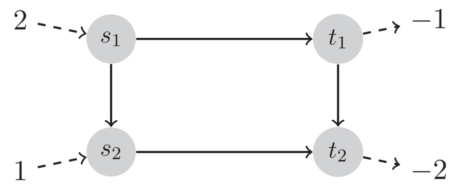

FIGURE 3 The graph shows that Theorem 16 does not hold for $|\mathcal{V}_+|, |\mathcal{V}_-| \geq 2$: Suppose that $b_{s_2}, b_{t_2} \neq 0$ and $b_{s_2} < -b_{t_2}$, then the flow on at least one of the arcs (s_1, s_2) and (t_1, t_2) has to be positive. Nevertheless, if $b_{t_1} \neq 0$, they need not be used in $\mathcal{P}^{\text{AS}\pm}$, that is, $\mathcal{P}^{\text{AS}\pm} \nsubseteq \mathcal{P}^{\text{AF}}$

Starting at node v, by the constraints (9c) and (9d), there exists an outgoing arc $a_1 = (v, v_1) \in \mathcal{A}(z^+, z^-)$ for some node $v_1 \in \mathcal{V} \setminus \{v\}$. Repeating this argument produces a path $(v, v_1, v_2, \dots, v_k)$ in $\mathcal{A}(z^+, z^-)$ until $v_k \in \mathcal{V}_-$. This process terminates, since the graph is finite and we cannot produce cycles. Similarly, going backward from u, by (9a) and (9b) there exists an arc $(u_1, u) \in \mathcal{A}(z^+, z^-)$ for some $u_1 \in \mathcal{V} \setminus \{u\}$. Repeating yields a path $(u_r, \dots, u_1, u)$ until $u_r \in \mathcal{V}_+$.

If $b \neq 0$, by (8a) there exists at least one path leaving each node in $\mathcal{V}_+$ and by (8b) there exists at least one path entering each node in $\mathcal{V}_-$.

Finally, let $b = 0$. Then there are no sources and sinks, that is, the construction above would either terminate at a node with degree 1 or produce a cycle, which contradicts either (9) or (11). Thus, $\mathcal{P}^{\text{AS}\pm} = \{0\}$ if $b = 0$. ■

Note that Proposition 14 recovers the essence of [3, Proposition 1], but there are minor differences: On the one hand, Proposition 14 can be applied to graphs that are not ASTS-orientable, allowing inner nodes of degree 1 in the graph whereas transshipment nodes of ASTS-orientable graphs need to have at least degree 2; however, a graph $\mathcal{D}(z^+, z^-)$ with $(z^+, z^-) \in \mathcal{P}^{\text{AS}\pm}$ is ASTS-orientable because Proposition 14 implies condition (ii) of [3, Theorem 1] after removing isolated nodes. On the other hand, [3, Proposition 1] also proves the existence of so-called supersources and -sinks.

We obtain the following first consequence:

Corollary 15. *For every balanced supply and demand vector b the polytopes $\mathcal{P}^{\text{AF}}$ and $\mathcal{P}^{\text{AS}\pm}$ satisfy the inclusion*

$$\mathcal{P}^{\text{AF}} \subseteq \mathcal{P}^{\text{AS}\pm}.$$

Proof. In the case $b = 0$, we have $\mathcal{P}^{\text{AS}\pm} = \mathcal{P}^{\text{AF}} = \{0\}$. Hence, we only have to consider the case $b \neq 0$. Furthermore, note that it suffices to prove the inclusion for all integer points.

Let $(z^+, z^-) \in \mathcal{P}^{\text{AF}} \cap \{0, 1\}^{2\mathcal{A}}$ with corresponding acyclic b-flow $x \in \mathbb{R}^{\mathcal{A}}$. By assumption $b \neq 0$, flow x is nonzero. This implies that there is at least one path with nonzero flow leaving each node in $\mathcal{V}_+$ and at least one path with nonzero flow entering each node in $\mathcal{V}_-$. Thus, the constraints (8) are satisfied. Due to flow conservation, the inequalities (9a)–(9d) hold. Moreover, since x is acyclic, (11) is satisfied. Hence, we have $(z^+, z^-) \in \mathcal{P}^{\text{AS}\pm}$ which concludes the proof. ■

Figure 3 shows that $\mathcal{P}^{\text{AF}} = \mathcal{P}^{\text{AS}\pm}$ does not hold in general, since $\mathcal{P}^{\text{AS}\pm}$ does not capture the amount of supply or demand. However, the following result characterizes a special case such that equality holds.

Theorem 16. *Suppose that $|\mathcal{V}_+| = 1$ or $|\mathcal{V}_-| = 1$ if $b \neq 0$. Then, if there are no flow bounds,*

$$\mathcal{P}^{\text{AS}\pm} = \mathcal{P}^{\text{AF}}.$$

Proof. In the case $b = 0$, we have $\mathcal{P}^{\text{AS}\pm} = \mathcal{P}^{\text{AF}} = \{0\}$. Hence, we only have to consider the case $b \neq 0$. By the previous corollary it suffices to prove that the inclusion $\mathcal{P}^{\text{AS}\pm} \subseteq \mathcal{P}^{\text{AF}}$ is true. Note again that it suffices to prove the inclusion for all integer points. Moreover, we only consider the single-sink case $\mathcal{V}_- = \{t\}$, since the single-source case is analogous.

Let $(z^+, z^-) \in \mathcal{P}^{\text{AS}\pm} \cap \{0, 1\}^{2\mathcal{A}}$ and denote the sources with $\mathcal{V}_+ = \{s_1, \dots, s_k\}$. We first construct an acyclic flow $x \in \mathbb{R}^{\mathcal{A}}$ with $x_a < 0$ if $z_a^- = 1$, $x_a > 0$ if $z_a^+ = 1$, and $x_a = 0$ otherwise. By scaling, we will obtain a b-flow.

We start with the zero-flow $x = 0$ and define $\mathcal{P}_1 = \dots = \mathcal{P}_k = \emptyset$. We then pick an arc $a' \in \mathcal{A}$ with either $z_{a'}^+ = 1$ or $z_{a'}^- = 1$ and $x_{a'} = 0$. Then by Proposition 14 there exists a path P from a source s_i to the sink t in $\mathcal{D}(z^+, z^-)$ containing a' if $z_{a'}^+ = 1$ or otherwise $\overleftarrow{a}'$ if $z_{a'}^- = 1$. We add P to the set $\mathcal{P}_i$ and augment x along P by one unit, by increasing x_a by 1 for every arc $a \in \mathcal{A} \cap P$ and decreasing x_a by 1 for every arc $a \in \mathcal{A}$ such that $\overleftarrow{a} \in P$. For $a \in \mathcal{A}$ we define $\Delta(P)_a = 1$ if $a \in P$ and $\Delta(P)_a = -1$ if $\overleftarrow{a} \in P$ and $\Delta(P)_a = 0$ otherwise. Then the new flow is $x + \Delta(P)$. Since $\mathcal{A}(z^+, z^-)$ does not contain both a' and $\overleftarrow{a}'$, flow $x_{a'}$ can only be increased if $a' \in \mathcal{A}(z^+, z^-)$ or otherwise decreased if $\overleftarrow{a}' \in \mathcal{A}(z^+, z^-)$ by augmenting flow along another path, even for another source–sink pair. Therefore, we can iterate augmenting flow for the remaining arcs with no flow and thereby construct a flow with the desired flow directions. Note that

$$x = \sum_{i=1}^{k} \sum_{P \in \mathcal{P}_i} \Delta(P).$$

We still have to scale the flow such that it is a b-flow. First note that there might exist an index $i \in [k] = \{1, \dots, k\}$ with $\mathcal{P}_i = \emptyset$; for example, if the graph $\mathcal{D}$ itself is a path with the ends s_1 and t. Then, if we start the procedure above with a' incident to s_1, we only augment flow once and $\mathcal{P}_i = \emptyset$ for all $i > 1$. Hence, consider $i \in [k]$ with $\mathcal{P}_i = \emptyset$. By Proposition 14 there exists an s_i–t-path P in $\mathcal{D}(z^+, z^-)$. Then set $\mathcal{P}_i = \{P\}$.

We now define the scaled flow

$$\sum_{i=1}^{k} \frac{b_{s_i}}{|\mathcal{P}_i|} \sum_{P \in \mathcal{P}_i} \Delta(P).$$

Since b_{s_i} and $|\mathcal{P}_i| > 0$, the scaling is valid, does not change flow directions, and yields a b-flow. ∎

Remark 17. Figure 3 shows that Theorem 16 does not hold with more than one source and sink.

Proposition 14 also helps to determine the structure of integer points in $\mathcal{P}^{\mathrm{AS}\pm}$. For a subset $S \subseteq \overleftrightarrow{\mathcal{A}}$, let $\chi(S)$ be the *incidence vector* $(\chi^-, \chi^+) \in \{0,1\}^{2\mathcal{A}}$ defined by $\chi_a^+ = 1$ if $a \in S \cap \mathcal{A}$, $\chi_{\overleftarrow{a}}^- = 1$ if $\overleftarrow{a} \in S \cap \overleftarrow{\mathcal{A}}$ and 0 otherwise.

Corollary 18. *Each integer point $(z^+, z^-) \in \mathcal{P}^{\mathrm{AS}\pm}$ is the incidence vector of a union of source–sink-paths in $\overleftrightarrow{\mathcal{D}}$ that does not contain cycles and conversely.*

Proof. For each $a \in \mathcal{A}(z^+, z^-)$ there exists a source–sink-path P_a in $\mathcal{A}(z^+, z^-)$ that contains a by Proposition 14. Then each arc in $\mathcal{A}(z^+, z^-)$ is covered by $\cup_a P_a$ and the union does not contain cycles. Thus $(z^+, z^-) = \chi(\cup_a P_a)$.

Conversely, the incidence vectors of a union of source–sink-paths that does not contain cycles clearly satisfies (8), (9), as well as (11) and is therefore contained in $\mathcal{P}^{\mathrm{AS}\pm}$. ∎

Note that Corollary 18 is similar to [3, Proposition 1]. Moreover, note that the union of source–sink-paths can contain cycles, even in the single-source and -sink case; see the example in Figure 1.

Another consequence of Proposition 14 is that z_a^+ and $z_{\overleftarrow{a}}^-$ can be fixed to 0 or 1 in some cases, as we will discuss next. This provides bounds on the dimension of $\mathcal{P}^{\mathrm{AS}\pm}$.

We first need the following definition. Recall that we assume that $\mathcal{D}$ is weakly connected and consider two arcs a_1 and $a_2 \in \mathcal{D}$ such that neither is a bridge and $\mathcal{D} - \{a_1, a_2\}$ has exactly two weakly connected components $\mathcal{D}_1$ and $\mathcal{D}_2$. Then $\{a_1, a_2\}$ is called a *cut–pair*. Assume that $\mathcal{D}_2$ contains neither source nor sink and that a_1 enters and a_2 leaves $\mathcal{D}_2$ (by reorientation). We call $\mathcal{D}_2$ *input–output subgraph*. Note that $\mathcal{D}_2$ might have no arcs, in which case a_1 and a_2 form a directed path.

Lemma 19. *Let $\mathcal{D}$ be the given weakly connected, simple digraph with sources $\mathcal{V}_+$ and sinks $\mathcal{V}_-$. Then the following holds for every $(z^+, z^-) \in \mathcal{P}^{\mathrm{AS}\pm}$.*

1. *If there is no source–sink-path in $\overleftrightarrow{\mathcal{D}}$ containing $a \in \mathcal{A}$ ($\overleftarrow{a} \in \overleftarrow{\mathcal{A}}$) then $z_a^+ = 0$ ($z_{\overleftarrow{a}}^- = 0$).*
2. *Let $a \in \mathcal{A}$ be a bridge, that is, $\mathcal{D} - a$ is not weakly connected, and let the two connected components of $\mathcal{D} - a$ be induced by B_1, B_2 with $\mathcal{V} = B_1 \dot\cup B_2$. Then the following holds for each of the two connected components $\mathcal{D}[B_i]$, $i = 1, 2$:*
   - (a) *Assume $B_i \cap \mathcal{V}_+ = \emptyset$ and $B_i \cap \mathcal{V}_- = \emptyset$. Then $z_{\overleftarrow{a}}^- = z_a^+ = 0$. Furthermore, $z_{\overleftarrow{a'}}^- = z_{a'}^+ = 0$ holds for all arcs in the induced subgraph $a' \in \mathcal{D}[B_i]$.*
   - (b) *Assume $B_i \cap \mathcal{V}_+ \neq \emptyset$ and $B_i \cap \mathcal{V}_- = \emptyset$. If $a \in \delta^+(B_i)$, then $z_a^+ = 1$ and if $a \in \delta^-(B_i)$, then $z_{\overleftarrow{a}}^- = 1$ holds.*
   - (c) *Assume $B_i \cap \mathcal{V}_+ = \emptyset$ and $B_i \cap \mathcal{V}_- \neq \emptyset$. If $a \in \delta^+(B_i)$, then $z_{\overleftarrow{a}}^- = 1$ and if $a \in \delta^-(B_i)$, then $z_a^+ = 1$ holds.*
3. *Let there exist an input–output subgraph of $\mathcal{D}$ with entering arc a and leaving arc a'. Then $z_a^+ = z_{a'}^+$ and $z_{\overleftarrow{a}}^- = z_{\overleftarrow{a'}}^-$.*

Proof. In all cases, it suffices to consider integer points $(z^+, z^-) \in \mathcal{P}^{\mathrm{AS}\pm}$, since the statement then holds for the convex hull $\mathcal{P}^{\mathrm{AS}\pm}$.

1 Suppose that there is no source–sink-path in $\overleftrightarrow{\mathcal{D}}$ containing a ($\overleftarrow{a}$). By Proposition 14, $\mathcal{A}(z^+, z^-)$ cannot contain a ($\overleftarrow{a}$). Thus, $z_a^+ = 0$ ($z_{\overleftarrow{a}}^- = 0$).

2 In case (2a), B_i contains neither a source nor a sink. Since the paths are simple and $\mathcal{D}(z^+, z^-)$ is acyclic, no path can enter B_i. In case (2b), at least one source–sink-path has to enter B_i. In case (2c), at least one source–sink-path has to leave B_i.

3 Every union of source–sink-paths using a_1 also has to use a_2. This implies the given equations. ∎

Remark 20.

1 The results in Lemma 19 are similar to the ones by Becker and Hiller [3, 4], but in a different notation.
2 The existence of a node of degree 2 is a special case of Part 3 of Lemma 19.
3 It is an open question whether the affine hull of $\mathcal{P}^{\mathrm{AS}\pm}$ is completely characterized by the three conditions of Lemma 19; but see Proposition 29 for the single-source and -sink case.

A natural question is how the conditions in Lemma 19 can be checked. It turns out that the condition of Part 1 is hard to check, even for the single-source and -sink case.

Proposition 21. *Given a directed graph with source node s, sink node t and some arc $a = (u, v)$, it is NP-complete to decide whether there exists a (simple) s–t-path that contains a.*

Proof. Consider the k-vertex disjoint paths problem, which consists of finding vertex disjoint paths from s_i to t_i for a given set of node pairs $(s_1, t_1), \dots, (s_k, t_k)$. Obviously, finding an s–t-path that uses a is the special case of finding 2-vertex disjoint paths between (s, u) and (v, t). Fortune et al. [11] proved that the vertex disjoint paths problem on general directed graphs is NP-complete even for fixed $k \geq 2$. ■

Corollary 22. *Linear optimization over $\mathcal{P}^{\mathrm{AS}\pm}$ is NP-hard, even if there is a single source s and sink t.*

Proof. Consider the linear function that maximizes z_a^+ for some arc a over $\mathcal{P}^{\mathrm{AS}\pm}$. The optimal value is 1 if and only if there exists an s–t-path through a. The results then follows by NP-hardness of determining the latter by Proposition 21 ■

Remark 23. Schrijver [38] showed that for fixed k and planar graphs, an s–t-path that contains a given arc can be found in polynomial time. Recently, Fakcharoenphol et al. [10] showed that one can compute the set of all arcs that are not contained in an s–t-path of a planar graph in linear time.

Remark 24. With respect to Parts 2 and 3 of Lemma 19 the following holds. Bridges in graphs can be found in linear time; see Tarjan [42]. Moreover, checking whether a source and sink are in the same connected component can be done by breadth-first search in linear time; see, for example, Korte and Vygen [25]. Moreover, after bridges have been removed, the linear time algorithm of Mehlhorn et al. [30] outputs a cut–pair if one exists. More input–output subgraphs can be produced using this algorithm iteratively.

3.9 | Analysis of the single-source and -sink case

Since a complete understanding of $\mathcal{P}^{\mathrm{AS}\pm}$ in the general case seems to be hard to obtain, we provide a further analysis for the special case of a single source s and sink t in this section. This implies that the balanced $b \in \mathbb{R}^{\mathcal{V}}$ satisfies $b_s = -b_t \geq 0$ and $b_v = 0$ for all $v \in \mathcal{V} \setminus \{s, t\}$. To simplify notation, we orient the arcs incident to the source s and sink t such that $\delta^-(s) = \emptyset$ and $\delta^+(t) = \emptyset$ holds.

Lemma 25. *Let $\mathcal{D}$ be the given weakly connected, simple digraph with source s and sink t. Then for every $(z^+, z^-) \in \mathcal{P}^{\mathrm{AS}\pm}$, $z_a^- = 0$ holds for every $a \in \delta^+(s)$ and for every $a \in \delta^-(t)$.*

Proof. First consider an integer point $(z^+, z^-) \in \mathcal{P}^{\mathrm{AS}\pm}$. Assume the statement does not hold, and let $a = (s, v)$ with $z_a^- = 1$. Then going backward from v similarly to the proof of Proposition 14, there exists an s–v-path. This would close a cycle, hence, $z_a^- = 0$ holds for all $a \in \delta^+(s)$. For $a \in \delta^-(t)$ we can argue analogously. Since $\mathcal{P}^{\mathrm{AS}\pm}$ is the convex hull of the integer points, the statement holds. ■

Remark 26. Let $S \subset \mathcal{V}$ with $s \in S$, $t \notin S$ and consider the s–t-cut inequalities

$$z^+(\delta^+(S)) + z^-(\delta^-(S)) \geq 1.$$

Because of Corollary 18 these inequalities are valid for all integer points in $\mathcal{P}^{\mathrm{AS}\pm}$ and thus for their convex hull. However, they are weaker than the inequalities (8) and (9). Indeed, the s–t-cut inequalities together with nonnegativity provide a complete linear description of the dominant of the s–t-path polytope; see, for example, Schrijver [39, Theorem 13.1]. Moreover, as an example consider the incidence vector of the union of (at least) one s–t-path and some node-disjoint arc. This vector is feasible for the s–t-cut inequalities, but not for (8) and (9). However, these inequalities can be strengthened as follows.

Lemma 27. *Let $\mathcal{D}$ be a simple connected digraph with source s and sink t. Let $S \subset \mathcal{V}$ with $s \in S$, $t \notin S$. Then the inequalities*

$$z^+(\delta^+(S)) + z^-(\delta^-(S)) \geq 1 + z_a^- \qquad \forall a \in \delta^+(S), \tag{13a}$$

$$z^+(\delta^+(S)) + z^-(\delta^-(S)) \geq 1 + z_a^+ \qquad \forall a \in \delta^-(S) \tag{13b}$$

are valid for $\mathcal{P}^{\mathrm{AS}\pm}$.

Proof. Inequality (13a) is satisfied by all solutions in $\mathcal{P}^{\mathrm{AS}\pm}$ with $z_a^- = 0$ by Remark 26. Let $(z^+, z^-) \in \mathcal{P}^{\mathrm{AS}\pm}$ be an integral solution with $z_a^- = 1$. By Proposition 14, $\mathcal{D}(z^+, z^-)$ contains an s–t-path P that uses $\overleftarrow{a}$. Then P has to cross the cut at least twice and therefore $z^+(\delta^+(S)) + z^-(\delta^-(S)) \geq 2$. Thus, (13a) holds for the convex hull of these integer points, that is, $\mathcal{P}^{\mathrm{AS}\pm}$. The validity of (13b) can be seen similarly. ∎

Remark 28. Note that (13a) for $S = \{s\}$ yields (8a), since $z_a^- = 0$ for all $a \in \delta^+(s)$ by Lemma 25.

We can prove the following concerning the affine hull of $\mathcal{P}^{\mathrm{AS}\pm}$.

Proposition 29. *Assume that in $\overleftrightarrow{\mathcal{D}}$ there exist two arc-disjoint s–t-paths and for every arc $a \in \overleftrightarrow{\mathcal{A}} \setminus \{\overleftarrow{a} \ : \ a \in \delta^+(s) \cup \delta^-(t)\}$, there exist two s–t-paths containing a that are arc-disjoint except for the arc a itself. Then*

$$\dim \mathcal{P}^{\mathrm{AS}\pm} = |\overleftrightarrow{\mathcal{A}}| - \deg(s) - \deg(t),$$

where δ^+, δ^- and deg *are with respect to the original digraph $\mathcal{D}$.*

Proof. Consider an equation $(c^+)^\top z^+ + (c^-)^\top z^- = \gamma$ that is valid for $\mathcal{P}^{\mathrm{AS}\pm}$, that is, we have $\mathcal{P}^{\mathrm{AS}\pm} \subset \{(z^+, z^-) \ : \ (c^+)^\top z^+ + (c^-)^\top z^- = \gamma\}$. Let $c = (c^+, c^-)$.

By assumption there exist two arc-disjoint s–t-paths P_1 and P_2. Then the incidence vectors $\chi(P_1)$, $\chi(P_2)$, and $\chi(P_1 \cup P_2)$ are contained in $\mathcal{P}^{\mathrm{AS}\pm}$. Thus, the equalities $c^\top \chi(P_1) = c^\top \chi(P_2) = \gamma$ and $c^\top \chi(P_1 \cup P_2) = c^\top \chi(P_1) + c^\top \chi(P_2) = \gamma$ hold. Adding the first two equations yields $c^\top \chi(P_1) + c^\top \chi(P_2) = 2\,\gamma$ which implies $\gamma = 0$.

Consider an arbitrary arc $a \in \overleftrightarrow{\mathcal{A}} \setminus \{\overleftarrow{a} \ : \ a \in \delta^+(s) \cup \delta^-(t)\}$. By assumption there exist two s–t-paths P_1 and P_2 that are arc-disjoint, except for a. Let $\hat{P}_1 := P_1 \setminus \{a\}$ and $\hat{P}_2 := P_2 \setminus \{a\}$. Then for $i \in \{1, 2\}$ we get

$$c^\top \chi(P_i) = c^\top \chi(\hat{P}_i) + c_a = 0 \tag{14}$$

and moreover

$$c^\top \chi(P_1 \cup P_2) = c^\top \chi(\hat{P}_1) + c^\top \chi(\hat{P}_2) + c_a = 0$$

holds. Adding Equation (14) for $i \in \{1, 2\}$ yields

$$c^\top \chi(\hat{P}_1) + c^\top \chi(\hat{P}_2) + 2\,c_a = 0.$$

This implies $c_a = 0$, and therefore $c_a = 0$ for all arcs $a \in \overleftrightarrow{\mathcal{A}} \setminus \{\overleftarrow{a} \ : \ a \in \delta^+(s) \cup \delta^-(t)\}$. Thus, the only possible equations are the ones of Lemma 25, that is, $z_a^- = 0$ for all arcs $a \in \delta^+(s) \cup \delta^-(t)$, and linear combinations of them. Since the equations $z_a^- = 0$ for all arcs $a \in \delta^+(s) \cup \delta^-(t)$ are linearly independent, they reduce the dimension by $|\delta^-(s)| + |\delta^+(t)|$, which shows the claim. ∎

Note that due to the assumptions, Proposition 29 cannot be applied to graphs containing bridges or input–output subgraphs as mentioned in Lemma 19; see Figure 4 for a graph to which Proposition 29 can be applied. We are not aware of weaker conditions that still allow to compute the dimension of $\mathcal{P}^{\mathrm{AS}\pm}$ in general. Moreover, note that the assumptions also do not allow for the existence of an s–t-arc, since the only s–t-path using this arc would be the arc itself. Nevertheless, we could allow the existence of an s–t-arc, but then, if $(s, t) \in \overleftrightarrow{\mathcal{A}}$, the formula would have to be $\dim \mathcal{P}^{\mathrm{AS}\pm} = |\overleftrightarrow{\mathcal{A}}| - \deg(s) - \deg(t) + 1$ due to double counting.

Example 30. Consider again the graph given in Figure 2. This example shows that the LP-relaxation $\mathcal{P}_{\mathrm{LP}}^{\mathrm{AS}\pm}$ is not integral, that is, $\mathcal{P}^{\mathrm{AS}\pm} \subsetneq \mathcal{P}_{\mathrm{LP}}^{\mathrm{AS}\pm}$. Indeed, Figure 5 depicts a graph associated with a vertex of $\mathcal{P}_{\mathrm{LP}}^{\mathrm{AS}\pm}$.

Example 31. Again consider the graph in Figure 2 with $b_s = -b_t > 0$ and $b_v = b_u = 0$. Lemma 25 implies that

$$z_1^- = z_2^- = z_4^- = z_5^- = 0$$

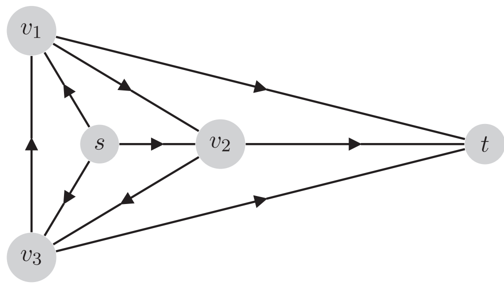

FIGURE 4 A simple graph fulfilling the assumptions of Proposition 29

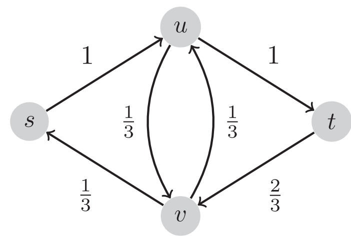

FIGURE 5 The graph $\mathcal{D}(z^+, z^-)$ associated with a vertex of $\mathcal{P}_{\mathrm{LP}}^{\mathrm{AS}\pm}$ applied to the network of Figure 2

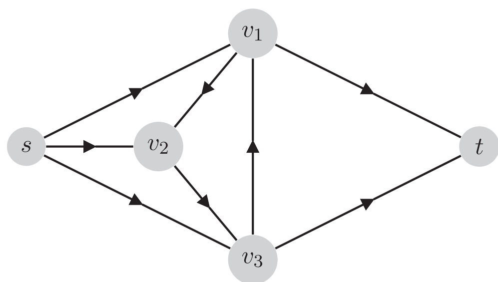

FIGURE 6 A graph for which dicycle inequalities (11) define facets of $\mathcal{P}^{\mathrm{AS}\pm}$

holds for all points in $\mathcal{P}^{\mathrm{AS}\pm}$. Furthermore, the other variables can take either value and we can verify (e.g., by using polymake) that these equations define the affine hull. Thus, in this example we have $\dim \mathcal{P}^{\mathrm{AS}\pm} = |\overleftrightarrow{\mathcal{A}}| - |\delta^-(s)| - |\delta^+(t)|$, although the assumptions of Proposition 29 are not satisfied for arc 3.

Most facets of $\mathcal{P}^{\mathrm{AS}\pm}$ are already part of the defining system of $\mathcal{P}_{\mathrm{LP}}^{\mathrm{AS}\pm}$: the variable bounds $z_1^+, z_2^+, z_4^+, z_5^+ \leq 1$ and $z_3^-, z_3^+ \geq 0$, the inequalities $1 \leq z_1^+ + z_2^+$, $1 \leq z_4^+ + z_5^+$ (see (8a) and (8b)) and $z_3^- + z_3^+ \leq 1$ (see (11)), and the node conditions (9a)–(9d) at nodes u and v:

$$\begin{aligned} z_1^+ &\leq z_3^+ + z_4^+, & z_2^+ &\leq z_3^- + z_5^+ \\ z_3^- &\leq z_4^+, & z_3^- &\leq z_2^+, \\ z_3^+ &\leq z_1^+, & z_3^+ &\leq z_5^+, \\ z_4^+ &\leq z_1^+ + z_{3,}^- & z_5^+ &\leq z_2^+ + z_3^-. \end{aligned}$$

The only facets that are given by other inequalities are

$$\begin{aligned} 1 + z_3^- &\leq z_2^+ + z_3^+ + z_4^+, \\ 1 + z_3^+ &\leq z_1^+ + z_3^- + z_5^+, \end{aligned} \tag{15}$$

which arise from (13a) and (13b).

Example 32. Interestingly, in the previous example there are no facets defined by the dicycle inequalities (11). Note that this does not hold in general, for example, consider the graph in Figure 6. Here the dicycle inequalities defined by the cycles $\{(v_1, v_2), (v_2, v_3), (v_3, v_1)\}$ and $\{(v_1, v_3), (v_3, v_2), (v_2, v_1)\}$ define facets of $\mathcal{P}^{\mathrm{AS}\pm}$.

As a conclusion from the analysis, one can say that even determining the dimension of $\mathcal{P}^{\mathrm{AS}\pm}$ seems to be hard. This is also true for the single-source, single-sink case. Note that understanding the dimension of a polytope is one of the preconditions for analyzing its facets. Such knowledge can then be used for deriving strong relaxations. Although we are currently far from a thorough understanding the polyhedral structure of $\mathcal{P}^{\mathrm{AS}\pm}$, the computational results in the next section will show that adding binary direction variables and dicycle inequalities already provides a good speed-up.

4 | NUMERICAL RESULTS

To demonstrate the effect of our method to handle acyclic flows via $\mathcal{P}^{\mathrm{AS}\pm}$, we describe computational experiments for gas networks. As mentioned in the introduction, gas networks can contain additional active elements. We first very briefly describe how the elements of a gas network are handled in our experiments and refer to [24] and [33] for (much) more details on gas network optimization.

4.1 | Model implementation

Recall from Example 1 that in stationary gas transport, the potentials are the squares of the pressures at the nodes. Since some of the models of network elements other than pipes cannot be (linearly) expressed in terms of the potentials, our model includes pressure variables p_u for all nodes $u \in \mathcal{V}$, which are coupled with the potentials through the equation $p_u^2 = \pi_u$. To avoid unnecessary nonlinear equations, our model only contains the potential variables, where they are actually needed. Note that this was a modeling choice and one could also only introduce the pressure variables as needed.

- Pipes are handled in the way described in Example 1 with $\psi(x_a) = |x_a|\, x_a$ and the resistances given by

$$\beta_a = \left(\frac{4}{\pi}\right)^2 \frac{L_a}{D_a^5}\, R_s\, T_m\, z_m\, \lambda_a, \quad \lambda_a := (2\log_{10}\left(\frac{D_a}{k_a}\right) + 1.138)^{-2},$$

  where L_a and D_a are the length and diameter of the pipe $a = (u, v) \in \mathcal{A}$, respectively, R_s is the specific gas constant, T_m is the temperature (assumed to be constant), z_m is the constant z-factor, and λ_a is the friction coefficient using the formula of Nikuradse [31, 32], where k_a is the roughness of the pipe. The z-factor is computed using the formula of the American Gas Association

$$z(p, T) = 1 + 0.257\frac{p}{p_c} - 0.533\frac{p}{p_c}\frac{T_c}{T},$$

  see Králik et al. [26], where p_c and T_c denote the pseudocritical pressure and pseudocritical temperature of the gas. Then $z_m := z(p_m, T_m)$ with the mean pressure value

$$p_m := \frac{1}{2}\max\{\underline{p}_u, \underline{p}_v\} + \frac{1}{2}\min\{\overline{p}_u, \overline{p}_v\}$$

  derived from the pressure bounds at nodes u and v.
- Valves control the gas flow. For open valves, the pressures on both sides are equal. For closed valves, the flow is 0 and the pressures are decoupled. These conditions are modeled using a binary variable in a straight-forward way.
- Compressors can increase gas pressure. Several compressors are often connected by piping and valves in compressor stations. We approximate the operation states of such stations by polyhedra in terms of flow, input and output pressure; see Hiller and Walther [22]. The operation modes of compressors are modeled using binary variables: the compressor can be turned on/off or it can be in bypass, that is, flow can bypass the compressor or can flow in the opposite direction. The possible modes are: compressor on/bypass closed, compressor off/bypass open and compressor off/bypass closed.
- Control valves, resistors, and short pipes are modeled as described in [24] and [33].
- As objective function we chose the maximization of the sum of pressures. Several other objective choices exist; see, for example, [18, 19]. Moreover, the computational results for other objective functions in [18] show a similar impact of our combinatorial models as seen here.

Since the flow conservation holds for all nodes and all adjacent arcs independently if the arcs are pipes or other network elements, the binary representation of flow conservation given by the inequalities (8) and (9) can be applied to the whole network. Therefore, we add the variables z_a^+, z_a^- for all arcs a except for compressor stations and control valves and couple them with the flows by using the linear relaxation (5) instead of (3). Moreover, since compressor stations and control valves are one-directional elements, that is, flow on such arcs is nonnegative, and their models already contain binary variables z_{cs} and z_{cv} indicating if they are active and if positive flow is possible, we use these variables as flow direction variables instead of additionally introducing z_a^+, which would be equal to z_{cs} or z_{cv}, and z_a^-, which could be fixed to 0 anyway. Depending on the model variant, we add inequalities (8) and (9)—except redundant cases, for example, in which flow on compressor stations and control valves is nonnegative.

Besides coupling the flow direction variables with the flows, they can be integrated in some of the network elements in a straightforward way. For all pipes $a = (u, v) \in \mathcal{A}$ they are coupled with the pressure variables by inequality

$$(\underline{p}_u - \overline{p}_v) z_a^- \leq p_u - p_v \leq (\overline{p}_u - \underline{p}_v) z_a^+.$$

Moreover, the binary variables for valves are coupled with the direction variables, such that $z_a^+ = z_a^- = 0$ if the valve is closed.

It is also possible to include the elements besides pipes in the dicycle inequalities (11). Resistors and control valves decrease the pressure in the direction of the flow and, thus, there can be no flow in a cycle including resistors or control valves. There is no pressure decrease in valves and short pipes and, hence, flow in a cycle consisting of only such arcs would be possible but unrealistic. Furthermore, flow in cycles including valves/short pipes and at least one pipe/resistor/control valve is still not possible by the same arguments as before. Last but not least, compressor stations increase the pressure, which makes flow in a cycle actually possible. However, such cycles significantly increase the temperature of the gas. Since our models do not include control of the temperature, we decided to forbid flow in such cycles by the dicycle inequalities.

In our code the dicycle inequalities (11) can be added for a cycle basis or for all cycles of the complete graph including active elements. Therefore, a cycle basis is computed as follows: after computing a spanning tree of the underlying undirected graph by breadth-first search, each nontree arc defines a cycle in the basis. All possible combinations of (multiple) basis cycles are then enumerated. To this end, we iteratively (try to) combine a basis cycle with another cycle, which is either a basis cycle or already a combination of cycles. Thereby, two cycles can be combined into a new cycle, if their symmetric difference induces a connected subgraph in which all nodes have degree two. Note that the enumeration and checking if two cycles can be combined, takes only a fraction of a second for the networks considered here. We then add dicycle inequalities for all orientations of cycles which do not traverse a control valve or compressor station in reverse direction, since these are one-directional.

4.2 | Results

In order to test the effects of the different conditions we performed computations with the following model variants:

- **NFD** *no* binary variables to represent flow directions;
- **FDO** with binary variables, but no flow conservation or dicycle inequalities;
- **CB** dicycle inequalities (11) for a cycle basis;
- **AC** dicycle inequalities (11) for all cycles;
- **FLC** binary flow conservation (8) and (9);
- **FLC + CB** variant FLC plus dicycle inequalities for a cycle basis;
- **FLC + AC** variant FLC plus dicycle inequalities for all cycles.

We use instances GasLib-40 and GasLib-582 from the GasLib library of gas network instances [13, 37]. The GasLib-40 network has 40 nodes, 39 pipes, and six compressor stations. The GasLib-582 network has 582 nodes, 278 pipes, five compressor stations, 23 control valves, eight resistors, 26 valves, and 269 short pipes. In total there are 4227 different scenarios for network GasLib-582, arising from different distributions of the loads.

For the instance GasLib-40 the binary flow conservation constraints (8) and (9) lead to 60 additional constraints. Furthermore, we can directly fix 14 flow direction variables of arcs adjacent to a node of degree one. A cycle basis of this network contains six cycles and there are 10 cycles in total. These cycles correspond to 12 respectively 20 dicycle inequalities. For the instance GasLib-582 the binary flow conservation leads to ∼1700 constraints and 351 variable fixings for nodes of degree one. Note that the exact number of constraints depends on the scenario, that is, the supply and demand vector. Moreover, a cycle basis of network GasLib-582 consists of 28 cycles and we found 165 cycles in total. These cycles correspond to 49 respectively 199 dicycle inequalities.

The computations were performed on a cluster with 3.5 GHz Intel Xeon E5-1620 Quad-Core CPUs, having 32 GB main memory and 10 MB cache running Linux. We used SCIP 7.0.0 [40], see also Gamrath et al. [12], with a 1-h time limit, single threaded, and we used CPLEX-12.10.0 as LP-solver.

Since the GasLib-40 instance is rather small, the solving time for all models is less than a second (and hence not reported in detail). Thus, this does not allow to draw conclusions on the different model variants. Nevertheless, the instance gives insight on some advantages of using the flow direction variables. Table 1 shows statistics on the flow bounds of the pipes after presolving. We apply standard presolving as described in Achterberg [1] and Vigerske [43]. Column "#fixed flows" shows the number of pipes with fixed flow, column "#fixed dirs" the number of pipes with fixed flow direction, and columns "$\underline{x}_{\text{mean}}$" and "$\overline{x}_{\text{mean}}$" the mean arithmetic lower and upper bounds of the flows. While the number of fixed flows is the same for all models, and mainly depends on the graph and the position of sources and sinks, the number of fixed directions and the mean arithmetic flow bounds can be improved by using the flow direction variables. This is also illustrated by Figure 7, which compares models NFD and FLC + AC. The figure distinguishes pipes with fixed flow, fixed direction and the remaining pipes.

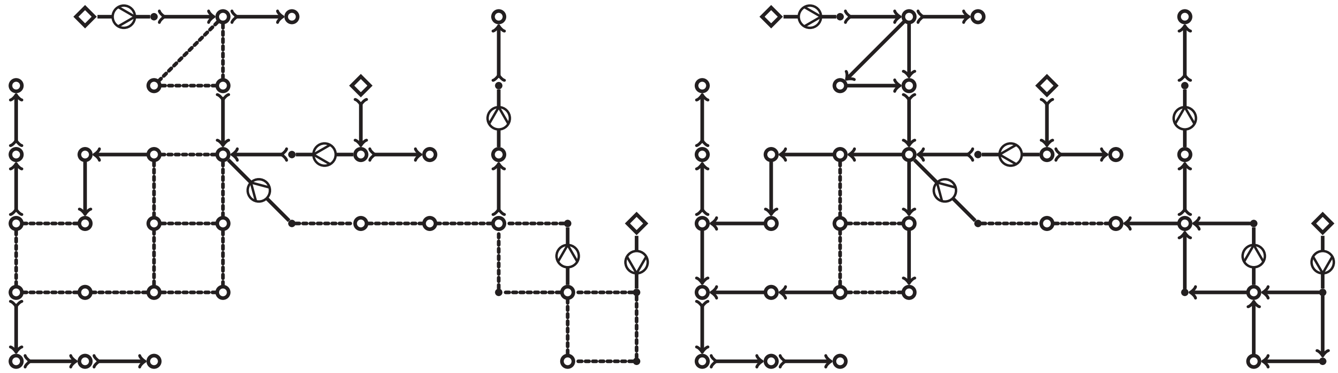

FIGURE 7 The presolved network GasLib-40 corresponding to variants NFD (left) and FLC + AC (right). The scenario has three sources (diamonds) and 29 sinks (circles). Pipes with fixed flow are depicted by ↣, fixed flow directions are shown by →, and the remaining pipes (with unfixed flows/directions) are dashed

TABLE 1 Statistics on the flow bounds after presolving of 39 pipes in network GasLib-40 for all model variants

Variant	#Fixed flows	#Fixed dirs	$\underline{x}_{\mathrm{mean}}$	$\overline{x}_{\mathrm{mean}}$
NFD	13	2	−189.23	245.10
FDO	13	12	−100.39	115.06
CB	13	17	−61.03	74.62
AC	13	17	−60.72	74.58
FLC	13	12	−98.25	111.73
FLC + CB	13	20	−41.39	54.33
FLC + AC	13	20	−41.24	54.33

TABLE 2 Aggregated results for GasLib582 scenarios for all model variants

Variant	Optimal	Feasible	Limit	Infeasible	Inf-presol
NFD	218	966	864	2179	2168
FDO	819	1223	6	2179	2168
CB	586	1454	8	2179	2168
AC	767	1278	3	2179	2174
FLC	1818	220	10	2179	2168
FLC + CB	1883	164	1	2179	2170
FLC + AC	2015	30	3	2179	2174

Note that we do not use optimality-based bound tightening (OBBT) in our experiments; see, for example, Gleixner et al. [15] and the references therein. Indeed, Becker and Hiller [4] used OBBT to further strengthen flow bounds.

The above results show that the mean arithmetic flow interval for model NFD is more than four times larger than the flow interval of model FLC + AC. Since tighter variable bounds typically lead to smaller branch-and-bound trees, this positive effect on the flow bounds will also be reflected in the solving times of large instances as can be seen by the following results for the GasLib-582 network.

The results of each model variant on the GasLib-582 network are given in Tables 2, 3, and 4 aggregated over all 4227 scenarios. In Table 2, column "optimal" gives the number of feasible scenarios solved to proven optimality, "feasible" the number of scenarios for which a feasible solution could be found, but could not be solved to optimality, "limit" the number of scenarios running into the time limit, "infeasible" the total number of scenarios that have been determined to be infeasible, and "inf-presol" the number of instances that have been determined to be infeasible during presolving.

Table 3 provides statistics for geometric mean times in seconds and the total running time in hours of the model variants. Here, column "to optimality" shows the geometric mean time over instances that could be solved to optimality, the column "to first" gives the geometric mean time until the first feasible solution was found taken of instances where this happened, "infeasible" the geometric mean time to prove infeasibility, "totalgeometric" the total geometric mean time over all scenarios, and "totaltime" shows the total computational time over all instances. Thereby, note that the total geometric mean time over all scenarios is much less than the time to optimality due to the running times of the infeasible scenarios.

TABLE 3 Geometric means of solving times in seconds and total run time in hours for all model variants for the GasLib582 scenarios

Variant	To optimality	To first	Infeasible	Totalgeometric	Totaltime (h)
NFD	1435.02	892.10	1.01	50.59	1948.68
FDO	1102.95	89.46	1.01	42.32	1553.21
CB	1209.24	81.65	1.01	45.76	1713.48
AC	1313.93	81.12	1.00	44.12	1627.08
FLC	549.28	113.09	1.01	23.69	641.43
FLC + CB	465.97	103.53	1.01	21.36	537.70
FLC + AC	290.98	68.04	1.00	15.94	270.28

TABLE 4 Statistics on the flow bounds after presolving of 278 pipes in network GasLib-582 for all model variants

Variant	#Fixed flows	#Fixed dirs	#Min dirs	#Max dirs	$\underline{x}_{\text{mean}}$	$\overline{x}_{\text{mean}}$
NFD	152.95	44.44	23	64	−111.03	174.98
FDO	152.41	50.35	25	83	−102.40	168.62
CB	151.87	52.81	25	87	−103.78	168.06
AC	152.43	53.14	25	104	−98.09	150.40
FLC	151.74	50.39	21	87	−103.41	166.69
FLC + CB	152.40	55.10	21	93	−94.53	162.76
FLC + AC	152.23	56.59	21	102	−84.63	135.68

In Table 4 similar statistics to Table 1 are given. Here, the results are averaged over all scenarios. Additionally, the columns "#min dirs" and "#max dirs" show the minimal and maximal number of fixed flow directions over all scenarios.

Remark 33. The numerical results shown in Table 2 are consistent in the sense that all variants identify the same 2179 infeasible scenarios. Moreover, for all other scenarios feasible solutions were found by at least one model variant. In fact, only 20 scenarios could not be solved to optimality. For these instances, at least one model variant found a feasible solution with optimality gap 0.4% or better.

The results clearly show that determining infeasibility seems to be easy in most cases. With all model variants, almost all infeasible scenarios could already be identified during presolving. That is, our acyclic flow models only slightly improve the computations here. However, the numbers for feasible scenarios show a completely different picture. Comparing the solving times in Table 3 for the basic model without any binary direction variables (i.e., NFD) with the model enhanced by $\mathcal{P}^{\text{AS}\pm}$ (i.e., FLC + AC) shows a speed-up factor of ~4.9 in geometric time to prove optimality, and a speed-up factor of ~7.2 in the total running times. Moreover, Table 2 shows that with model NFD no feasible solution has been found for almost half of the feasible scenarios, whereas with model FLC + AC almost all feasible scenarios could be solved to optimality.

A partial explanation for the performance improvement is as follows. Using the flow direction variables and the additional constraints, we can represent properties of feasible solutions, which are otherwise not included in the initial model or relaxation. Moreover, the heuristics and presolving techniques can detect more variable fixings, implications and reductions based on the flow conservation and the flow direction variables. For example, in diving heuristics, it is easier to detect infeasibility based on the binary flow direction variables without having to consider the nonlinear physics. This leads to tighter variable bounds (after presolving), which can be seen for the flow variables in Tables 1 and 4. Since having tight variables bounds is important to derive good relaxations for the nonlinearities, the LP-relaxations are already stronger early in the branch-and-bound tree. Moreover, tighter variable bounds (typically) lead to smaller branch-and-bound trees, since the search space is smaller. Indeed, we can observe this effect for the computations on the network GasLib-582. The arithmetic mean number of branch-and-bound nodes (rounded up) for the feasible scenarios solved to optimality with model variant NFD is 168 970, while it is 35 330 with model FLC + AC. That is, in model NFD it takes about 4.8 times as many nodes in comparison with variant FLC + AC, which is almost the same ratio as the speed-up for the geometric mean solving time to optimality shown in Table 3.

Another interesting observation is that variants AC and FLC form an exception of the positive effect of having tighter relaxations. Tables 1 and 4 both suggest that model variant AC defines the tighter LP-relaxation. Furthermore, also the geometric mean time until the first solution is found for the GasLib-582 scenarios is smaller with variant AC; see Table 3. However, with variant FLC more than twice the number of scenarios could be solved to optimality and also the geometric mean time to prove

TABLE 5 Aggregated results for GasLib582 scenarios for the ODE model

Variant	Optimal	Feasible	Limit	Infeasible	Inf-presol
NFD	41	93	2042	2051	2038
FLC + AC	1784	349	0	2094	2080

TABLE 6 Geometric means of solving times in seconds and total run time in hours for the GasLib582 scenarios for the ODE model

Variant	To optimality	To first	Infeasible	Totalgeometric	Totaltime (h)
NFD	864.49	1233.67	1.02	67.46	2149.23
FLC + AC	720.42	73.75	1.02	31.91	829.31

optimality is less than half. Thus, variant FLC seems to be better suited for optimization although AC yields tighter relaxations. However, combining the two variants performs even better.

Remark 34. The fact that potential-based flows are acyclic does not only hold for this algebraic model for stationary gas flows. It also applies to the stationary model based on ordinary differential equations used in [19]. Moreover, we also used variant CB and a preliminary version of FLC to derive the computational results there. The results for the ODE model show an even stronger effect of using the combinatorial models. In particular, results using variants NFD and FLC + AC can be seen in Tables 5 and 6. Note that for these computations, OBBT was used to strengthen bounds of the flow variables. Results for the other variants and the ODE model can be found in [18].

With model NFD, almost half of the scenarios ran into the time limit without a feasible solution. Only 41 scenarios could be solved optimally and feasible solutions were found for only 93 further scenarios. By contrast, with model FLC + AC all scenarios were either proven to be infeasible or a feasible solution was found. Moreover, 84% of the feasible instances were solved optimally.

5 CONCLUSIONS AND OPEN QUESTIONS

In this article we have investigated the usage of the property that potential-based flows are acyclic. We derived combinatorial models and investigated their properties. One of the main goals was to use these models to speed up optimization problems over potential-based flows. Indeed, our computational results show a speed-up of at least a factor of 3 if cycle information and knowledge on sources and sinks is used. The time to prove optimality shows a speed-up factor of almost 5, and the total running time speed-up of about 7.

In our computations we added the dicycle inequalities up front. It would be interesting to compare the performance of an algorithm that dynamically separates dicycle inequalities.

There are several open questions that we plan to investigate in the future. One open question is whether the conditions in Lemma 25 suffice to define the dimension of $\mathcal{P}^{\mathrm{AS}\pm}$, for example, in the planar case. Obtaining facets of $\mathcal{P}^{\mathrm{AS}\pm}$ would be interesting, in order to possibly further strengthen the formulation of potential-based flows. Such facets might be transferred from the acyclic subgraph polytope. This seems to be difficult, though. Moreover, it would be interesting to investigate whether the property of unique flows could be exploited in combinatorial models as well.

ACKNOWLEDGMENTS

This work was supported by the German Research Foundation (Deutsche Forschungsgemeinschaft, DFG) Research Grant CRC/Transregio 154 within Project A01. Furthermore, the authors thank three anonymous reviewers whose comments helped to improve the presentation of this article. Open access funding enabled and organized by Projekt DEAL.

ORCID

Marc E. Pfetsch https://orcid.org/0000-0002-0947-7193

REFERENCES

[1] T. Achterberg, Constraint integer programming, Ph.D. thesis, Technical Univ Berlin, 2007.

[2] B. Assarf, E. Gawrilow, K. Herr, M. Joswig, B. Lorenz, A. Paffenholz, and T. Rehn, *Computing convex hulls and counting integer points with polymake*, Math. Program. Comput. **9**(1) (2017), 1–38.
[3] K.-H. Becker and B. Hiller, ASTS orientations on undirected graphs: Structural analysis and enumeration. *ZIB-Report 18-31*, Zuse Institute Berlin, Berlin, Germany, 2018.
[4] K.-H. Becker and B. Hiller, Improved optimization models for potential-driven network flow problems via ASTS orientations. *ZIB-Report 19-58*, Zuse Institute Berlin, Berlin, Germany, 2019.
[5] K.-H. Becker and B. Hiller, Efficient enumeration of acyclic graph orientations with sources or sinks revisited. *ZIB-Report 20-05*, Zuse Institute Berlin, Berlin, Germany, 2020.
[6] D. Bienstock, Electrical transmission system cascades and vulnerability: An operations research viewpoint. *MOS-SIAM series on optimization*, SIAM, Philadelphia, PA, 2015.
[7] G. Birkhoff and J. B. Diaz, *Non-linear network problems*, Quart. Appl. Math. **13** (1956), 431–443.
[8] J. Burgschweiger, B. Gnädig, and M. C. Steinbach, *Optimization models for operative planning in drinking water networks*, Optim. Eng. **10**(1) (2009), 43–73.
[9] M. Collins, L. Cooper, R. Helgason, J. Kennington, and L. LeBlanc, *Solving the pipe network analysis problem using optimization techniques*, Manage. Sci. **24**(7) (1978), 747–760.
[10] J. Fakcharoenphol, B. Laekhanukit, and P. Sukprasert, *Finding all useless arcs in directed planar graphs*, arXiv preprint arXiv:1702.04786, 2018.
[11] S. Fortune, J. Hopcroft, and J. Wyllie, *The directed subgraph homeomorphism problem*, Theor. Comput. Sci. **10**(2) (1980), 111–121.
[12] G. Gamrath, et al., *The SCIP optimization suite 7.0*. Technical report, Optimization Online, 2020.
[13] GasLib *GasLib – A library of gas network instances*, Available at http://gaslib.zib.de/.
[14] E. Gawrilow and M. Joswig, *polymake: A framework for analyzing convex polytopes*, in Polytopes—Combinatorics and computation (Oberwolfach, 1997)*, volume 29 of DMV Sem*, Birkhäuser, Basel, Switzerland, 2000, 43–73.
[15] A. Gleixner, T. Berthold, B. Müller, and S. Weltge, *Three enhancements for optimization-based bound tightening*, J Glob Optim **67** (2017), 731–757.
[16] M. Groß, M. E. Pfetsch, L. Schewe, M. Schmidt, and M. Skutella, *Algorithmic results for potential-based flows: Easy and hard cases*, Networks **73**(3) (2019), 306–324.
[17] M. Grötschel, M. Jünger, and G. Reinelt, *On the acyclic subgraph polytope*, Math. Program. **33**(1) (1985), 28–42.
[18] O. Habeck, Mixed-integer optimization with ordinary differential equations for gas networks, Ph.D. thesis, Technische Universität Darmstadt, 2020.
[19] O. Habeck, M. E. Pfetsch, and S. Ulbrich, *Global optimization of mixed-integer ODE constrained network problems using the example of stationary gas transport*, SIAM J. Optim. **29**(4) (2019), 2949–2985.
[20] C. T. Hendrickson and B. N. Janson, *A common network flow formulation for several civil engineering problems*, Civil Eng. Syst. **1**(4) (1984), 195–203.
[21] B. Hiller and K. H. Becker, Improving relaxations for potential-driven network flow problems via acyclic flow orientations. *ZIB-Report 18-30*, Zuse Institute Berlin, Berlin, Germany, 2018.
[22] B. Hiller and T. Walther, Modelling compressor stations in gas networks. *Technical report 17-67*, Zuse Institut Berlin, Berlin, Germany, 2018.
[23] R. M. Karp, *Reducibility among combinatorial problems*, in *Complexity of computer computations*, R. Miller and J. Thatcher, Eds., Springer, Boston, MA, 1972, 85–103.
[24] T. Koch, B. Hiller, M. E. Pfetsch, and L. Schewe, Eds., Evaluating gas network capacities. *MOS-SIAM series on optimization*, Society for Industrial and Applied Mathematics, Philadelphia, PA, 2015.
[25] B. Korte and J. Vygen, Combinatorial optimization. Theory and algorithms*, volume 21 of Algorithms and combinatorics*, 6th ed., Springer, Heidelberg, Germany, 2018.
[26] J. Králik, P. Stiegler, Z. Vostrý, and J. Záworka, Dynamic modeling of large-scale networks with application to gas distribution*, volume 6 of* Studies in automation and control, Elsevier, Amsterdam, Netherlands, 1988.
[27] B. E. Larock, R. W. Jeppson, and G. Z. Watters, *Hydraulics of pipeline systems*, CRC Press, Boca Raton, FL, 2010.
[28] K. Lehmann, A. Grastien, and P. Van Hentenryck, *The complexity of DC-Switching problems*. Technical report 1411.4369, arXiv, 2014.
[29] J. J. Maugis, *Etude de réseaux de transport et de distribution de fluide*, RAIRO Oper. Res. **11**(2) (1977), 243–248.
[30] K. Mehlhorn, A. Neumann, and J. M. Schmidt, *Certifying 3-edge-connectivity*, Algorithmica **77**(2) (2017), 309–335.
[31] J. Nikuradse, Strömungsgesetze in rauhen Rohren. *Forschungsheft auf dem Gebiete des Ingenieurwesens*, VDI-Verlag, Düsseldorf, Germany, 1933.
[32] J. Nikuradse, Laws of flow in rough pipes*, Technical memorandum 1292*, National Advisory Committee for Aeronautics, Washington, DC, 1950.
[33] M. E. Pfetsch, A. Fügenschuh, B. Geißler, N. Geißler, R. Gollmer, B. Hiller, J. Humpola, T. Koch, T. Lehmann, A. Martin, A. Morsi, J. Rövekamp, L. Schewe, M. Schmidt, R. Schultz, R. Schwarz, J. Schweiger, C. Stangl, M. C. Steinbach, S. Vigerske, and B. M. Willert, *Validation of nominations in gas network optimization: Models, methods, and solutions*, Optim. Methods Softw. **30**(1) (2015), 15–53.
[34] A. U. Raghunathan, *Global optimization of nonlinear network design*, SIAM J. Optim. **23**(1) (2013), 268–295.
[35] R. Z. Ríos-Mercado, S. Wu, L. R. Scott, and E. A. Boyd, *A reduction technique for natural gas transmission network optimization problems*, Ann. Operat. Res. **117**(1) (2002), 217–234.
[36] R. T. Rockafellar, *Network flows and monotropic optimization*, 2nd ed., Athena Scientific, Belmont, MA, 1998.
[37] M. Schmidt, D. Aßmann, R. Burlacu, J. Humpola, I. Joormann, N. Kanelakis, T. Koch, D. Oucherif, M. E. Pfetsch, L. Schewe, R. Schwarz, and M. Sirvent, *GasLib–A library of gas network instances*, Data **2**(4) (2017), 40.
[38] A. Schrijver, *Finding k disjoint paths in a directed planar graph*, SIAM J. Comput. **23**(4) (1994), 780–788.
[39] A. Schrijver, Combinatorial optimization: Polyhedra and efficiency*, volume 24 of Algorithms and combinatorics*, Springer, New York, NY, 2003.
[40] SCIP *Solving constraint integer programs*, Available at http://scip.zib.de/.

[41] J. Szabó, The set of solutions to nomination validation in passive gas transportation networks with a generalized flow formula. *ZIB-Report 11-44*, Zuse Intitute Berlin, Berlin, Germany, 2012.
[42] R. E. Tarjan, *A note on finding the bridges of a graph*, Inf Process Lett **2**(6) (1974), 160–161.
[43] S. Vigerske, Decomposition in multistage stochastic programming and a constraint integer programming approach to mixed-integer nonlinear programming, Ph.D. thesis, Humboldt-Universität zu Berlin, 2013.

How to cite this article: Habeck O, Pfetsch ME. Combinatorial acyclicity models for potential-based flows. *Networks*. 2022;79:83–104. https://doi.org/10.1002/net.22038